# IMPURITY EFFECTS ON SUPERCONDUCTORS AND THE ELECTRON-PHONON INTERACTION

A THESIS
SUBMITTED TO THE DEPARTMENT OF PHYSICS
AND THE INSTITUTE OF ENGINEERING AND SCIENCE
OF BILKENT UNIVERSITY
IN PARTIAL FULFILLMENT OF THE REQUIREMENTS
FOR THE DEGREE OF
MASTER OF SCIENCE

BY
Kerim Savran
September 2000

# IMPURITY EFFECTS ON SUPERCONDUCTORS AND THE ELECTRON-PHONON INTERACTION

A THESIS

SUBMITTED TO THE DEPARTMENT OF PHYSICS

AND THE INSTITUTE OF ENGINEERING AND SCIENCE

OF BILKENT UNIVERSITY

IN PARTIAL FULFILLMENT OF THE REQUIREMENTS

FOR THE DEGREE OF

MASTER OF SCIENCE

By

Kerim Savran

September 2000

I certify that I have read this thesis and that in my opinion it is fully adequate, in scope and in quality, as a dissertation for the degree of Master of Science.

Assoc. Prof. Yong-Jihn Kim (Supervisor)

I certify that I have read this thesis and that in my opinion it is fully adequate, in scope and in quality, as a dissertation for the degree of Master of Science.

Asst. Prof. Zafer Gedik

I certify that I have read this thesis and that in my opinion it is fully adequate, in scope and in quality, as a dissertation for the degree of Master of Science.

Asst. Prof. Ulrike Salzner

Approved for the Institute of Engineering and Science:
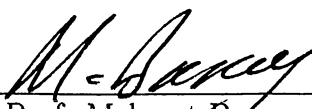
Prof. Mehmet Baray,
Director of Institute of Engineering and Science

# Abstract

## IMPURITY EFFECTS ON SUPERCONDUCTORS AND THE ELECTRON-PHONON INTERACTION

**Kerim Savran**

M. S. in Physics

Supervisor: Assoc. Prof. Yong-Jihn Kim

September 2000

In this thesis effects of impurities on superconductors and electron-phonon interactions in metals are studied.

The first part deals with the effect of magnetic impurities on superconductors. In particular, we focus on the experimental observation that the effect of magnetic impurities in a superconductor is drastically different depending on whether the host superconductor is in the crystalline or the amorphous state. Based on the recent theory of Kim and Overhauser, it is shown that as the disorder in the system increases, the initial slope of the $T_c$ depression decreases by a factor $\sqrt{\ell/\xi_0}$, when the mean free path $\ell$ becomes smaller than the BCS coherence length $\xi_0$, which is in agreement with experimental findings. Additionally, the transition temperature $T_c$ for a superconductor, which is in a pure crystalline state, drops sharply from about 50% of $T_{c0}$ (transition temperature of a pure system) to zero near the critical impurity concentration. This *pure limit behavior* was found in crystalline Cd by Roden and Zimmermeyer.

In the second part, the effect of weak localization on electron-phonon interactions in metals is investigated. As weak localization leads to the same

correction term to both conductivity and electron-phonon coupling constant $\lambda$ (and $\lambda_{tr}$), the temperature dependence of the thermal electrical resistivity is decreasing as the conductivity is decreasing due to weak localization. Consequently, the temperature coefficient of resistivity (TCR) decreases, while the residual resistivity increases. As the coupling constant $\lambda$ approaches zero, only the residual resistivity part remains and accordingly TCR becomes negative. In other words, the Mooij rule turned out to be a manifestation of weak localization correction to the conductivity and the electron-phonon interaction.

# Özet

## ÜSTÜNİLETKENLERDE SAFSIZLIK ETKİLERİ VE ELEKTRON-FONON ETKİLEŞİMLERİ

**Kerim Savran**
Fizik Yüksek Lisans
Tez Yöneticisi: Assoc. Prof. Yong-Jihn Kim
Eylül 2000

Bu çalışmada üstüniletkenlerdeki safsızlık etkileri ve elektron-fonon etkileşimi incelenmiştir.

İlk bölümde üstüniletkenlerde manyetik safsızlık etkileri ele alınmıştır. Özellikle, üstüniletkenin kristal ya da amorf yapıda olup olmamasına bağlı olarak manyetik safsızlıkların üstüniletkenler üzerindeki etkisinin farklı olmasının deneysel olarak incelenmesi üzerinde durmaktayız. Kim ve Overhauser'ın manyetik safsızlıkların üstüniletkenler hakkındaki teorileri baz alınıp $T_c$ eğrisinin başlangıçtaki eğiminin, sistemin düzensizliği artarken, $\sqrt{\frac{\ell}{\xi_0}}$ faktörü ile azaldığı gösterilmiştir. Öyle ki serbest hareket yolu $\ell$ BCS koherenz uzunluğundan ($\xi_0$) çok düşük olduğu durumda incelenen bu olay deneysel bulgularla uyum içerisindedir. Buna ek olarak üstüniletkenin kritik geçiş sıcaklığı $T_c$ kritik manyetik safsızlık değeri yakınlarında keskin bir düşüşle saf iletkenin kritik geçiş sıcaklığının ($T_{c0}$) yarısı olduğu değerden sıfıra inmektedir. Bu *saf limit davranışı* Roden ve Zimmermeyer tarafından kristal Cd için bulunmuştur.

İkinci bölümde, elektron-fonon etkileşimlerinde zayıf yerelleşme etkileri incelenmiştir. Zayıf yerelleşme hem iletkenlik, hem de elektron-fonon çiftlerinin katsayılarına aynı düzeltme terimlerinin etki etmesine yardımcı olduğu için ısıl elektrik direncinin sıcaklığa bağımlılığı azalmaktadır. Sonuç olarak özdirencin sıcaklık katsayısı (ÖSK) özdirenç artarken azalmaktadır. Çiftlenim katsayısı $\lambda$ sıfıra giderken sadece artık özdirenç kısım ve buna bağlı olarak ÖSK negatif olmaktadır. Başka bir deyişle Mooij kuralı iletkenlikte ve elektron-fonon etkileşimlerinde zayıf yerelleşmenin getirdiği düzeltmenin ortaya konmasıdır.

**Anahtar**
**sözcükler:** Üstüniletkenlik, elektron-fonon etkileşimi, manyetik safsızlık, zayıf yerelleşme, Mooij kuralı.

İkinci bölümde, elektron-fonon etkileşimlerinde zayıf yerelleşme etkileri incelenmiştir. Zayıf yerelleşme hem iletkenlik, hem de elektron-fonon çiftlerinin katsayılarına aynı düzeltme terimlerinin etki etmesine yardımcı olduğu için ısıl elektrik direncinin sıcaklığa bağımlılığı azalmaktadır. Sonuç olarak özdirencin sıcaklık katsayısı (ÖSK) özdirenç artarken azalmaktadır. Çiftlenim katsayısı $\lambda$ sıfıra giderken sadece artık özdirenç kısın ve buna bağlı olarak ÖSK negatif olmaktadır. Başka bir deyişle Mooij kuralı iletkenlikte ve elektron-fonon etkileşimlerinde zayıf yerelleşmenin getirdiği düzeltmenin ortaya konmasıdır.

**Anahtar**
**sözcükler:** Üstüniletkenlik, elektron-fonon etkileşimi, manyetik safsızlık,
zayıf yerelleşme, Mooij kuralı.

# Acknowledgement

I would like to express my deepest gratitude to *Assoc. Prof. Yong-Jihn Kim* for his supervision during research, guidance and understanding throughout this thesis.

I also wish to thank *Asst. Prof. Ulrike Salzner* as she helped me to refine the context of my thesis.

Feridun Ay and Sefa Dağ helped me do my technical work and also Özgür Çakır, Feridun Ay, İsa Kiyat, Selim Tanrıseven and M. Ali Can kept my spirits high all the time, thank you very much, I really appreciate it.

Last but not the least, I would like to thank my family.

# Contents

# List of Figures

# List of Tables

# Chapter 1

# Introduction

## 1.1 Introduction to Superconductivity

Superconductivity has been one of the most discussed phenomena of the last century.[1-5] Since Kammerling Onnes[6] first discovered the superconducting state of mercury in 1911, many scientists have worked on this phenomenon and many theories on microscopic and macroscopic scales were derived.

It is observed that if we cool a metal or an alloy below a critical temperature, usually denoted as $T_c$, a specific heat anomaly occurs. This is not due to a change in the crystallographic structure or in ferromagnetic or antiferromagnetic transitions. The cooled down substance has zero resistance. For instance, a current induced in a tin ring (cooled down below $T_c$=3.7K) persists longer than 1 year. This is why we call this state the superconducting state, and the persistent current is called supercurrent.

Another striking characteristic property of the superconducting state is that the superconductors expel magnetic field lines. This effect is called Meissner effect and first shown experimentally by Meissner and Ochsenfeld[7] in 1933. One can easily obtain the Meissner effect using the persistent current phenomenon and thermodynamic equilibrium.

There are two types of superconducting materials. Nontransition metals are called Type-1, or Pippard superconductors, while transition metals and

intermetallic compounds are called Type-2 or London superconductors.[8]

As mentioned above, there are several macroscopic and microscopic theories of superconductors. In order to explain the perfect conductivity and the Meissner effect, London[9] proposed two equations. A slightly different notation of the second London equation is $h + \lambda_L^2 \nabla \times (\nabla \times h) = 0$. In this equation he introduced the London penetration depth, $\lambda_L$. This equation helps us to calculate the distribution of fields and currents. (The Meissner effect follows directly as London equation is satisfied for Type-2 superconductors.)

Pippard[10] proposed a modification of the London equation on empirical grounds. The London equation is valid only if $\lambda_L \gg \xi_0$, where $\xi_0$ is the coherence length. The coherence length of a metal is directly proportional to the Fermi velocity, thus for nontransition metals, for which the penetration depth $\lambda_L$ is small ($\sim 300 \AA$) and the coherence length is large ($\cong 10^4 \AA$ for aluminum), the London equation does not apply. Nontransition metals do exhibit the Meissner effect but in order to calculate the penetration depth a more complicated equation was suggested by Pippard. The Pippard equation is

$$j(\mathbf{x}) = -\frac{3}{4\pi c \Lambda \xi_0} \int d^3\mathbf{y} \frac{\mathbf{r}(\mathbf{r} \cdot \mathbf{A}(\mathbf{y})) e^{-\frac{r}{\xi_0}}}{r^4}, \qquad (1.\ 1)$$

where $\Lambda$ is defined as $\frac{4\pi\lambda_L^2}{c^2}$, and r is $|\mathbf{x} - \mathbf{y}|$. For slowly varying $\mathbf{A}$, the Pippard expression reduces to the London equation.

Ginzburg and Landau[11] have constructed a theory of the phenomenonology of the superconducting state and of the spatial variation of the order parameter in that state. In the Ginzburg Landau equation an order parameter, $\psi(\mathbf{r})$ is introduced, where $\psi^*(\mathbf{r})\psi(\mathbf{r}) = n_s(\mathbf{r})$, is the local concentration of superconducting electrons. Then as the total free energy $\int dV F_s(\mathbf{r})$ is minimized with respect to variations in the order parameter, where $F_s(\mathbf{r})$ is free energy density, we obtain the Ginzburg-Landau equation, resembling a Schrödinger equation for $\psi$ :

$$[(\frac{1}{2m})(-i\hbar\nabla - \frac{q\mathbf{A}}{c})^2 - \alpha + \beta|\psi|^2]\psi = 0 \qquad (1.\ 2)$$

As we consider the microscopic theories about the superconductivity, we see

that Fröhlich[12] was the first to point out that the electron-phonon interaction initiates an effective attractive electron-electron interaction, which may be the cause of the existence of superconductivity. In order to obtain the famous Fröhlich Hamiltonian we may start with the Hamiltonian of a lattice of bare ions, whose mutual interaction would include the long-range Coulomb potential, and then add the electron gas which would shield the potential due to the ions. It is however possible to explore many of the consequences of the electron-phonon interaction by use of the following simpler model. In the second quantized form, the Fröhlich Hamiltonian can be written as:

$$
\begin{aligned}
H &= \sum_{\mathbf{k}} \varepsilon_{\mathbf{k}} c_{\mathbf{k}}^{+} c_{\mathbf{k}} + \sum_{\mathbf{q}} \hbar \Omega_{\mathbf{q}} (b_{\mathbf{q}}^{+} b_{\mathbf{q}} + \frac{1}{2}) + \sum_{\mathbf{k},\mathbf{q}} [g_{\mathbf{q}}^{*} b_{\mathbf{q}}^{+} c_{\mathbf{k}}^{+} c_{\mathbf{k}+\mathbf{q}} + h.c.] \\
&= \sum_{\mathbf{k}} \varepsilon_{\mathbf{k}}' c_{\mathbf{k}}^{+} c_{\mathbf{k}} + \sum_{\mathbf{q}} \hbar \Omega_{\mathbf{q}}' (b_{\mathbf{q}}^{+} b_{\mathbf{q}} + \frac{1}{2}) \\
&\quad + \sum_{\mathbf{k}\mathbf{k}'\mathbf{q}\sigma\sigma'} |g_{\mathbf{q}}|^{2} \frac{\hbar \Omega_{\mathbf{q}}'}{[\varepsilon_{\mathbf{k}+\mathbf{q}} - \varepsilon_{\mathbf{k}}]^{2} - (\hbar \Omega_{\mathbf{q}})^{2}} \times c_{\mathbf{k}+\mathbf{q},\sigma}^{+} c_{\mathbf{k}'-\mathbf{q},\sigma'}^{+} c_{\mathbf{k}',\sigma'} c_{\mathbf{k},\sigma}. \quad (1.\ 3)
\end{aligned}
$$

where $g_{q}$ are coupling parameters and can be taken as purely imaginary. Here $\varepsilon_{k}'$ and $\Omega_{q}'$ denote the renormalization of the electron energy and the phonon frequency due to the electron-phonon interaction.

The microscopic understanding of superconductivity was provided by the classic 1957 paper of Bardeen, Cooper and Schrieffer, known as BCS theory.[13] They showed that attractive Fröhlich interaction between electrons can lead to a ground state of Cooper pairs separated from the excited states by an energy gap. As a result, most extraordinary properties of superconductors, such as thermal and electromagnetic properties, are explained by the presence of this energy gap. Indeed, the Fröhlich's phonon mediated interaction leads to an energy gap of the observed magnitude, and the penetration depth and coherence length emerge naturally. The transition temperature of an element or alloy is determined by the BCS coupling constant $\lambda = N(E_{F})V$. Here $N(E_{F})$ is the density of states for one spin at the Fermi level and V is the phonon mediated matrix element, which can be estimated from the electrical resistivity at room temperature. Two fundamental equations of the BCS theory are the BCS reduced hamiltonian and

the gap equation which defines the gap energy between the excited state and the ground state. This gap equation may be written as

$$\Delta = \frac{\omega_D}{\sinh(1/N(E_F)V)} \cong 2\omega_D e^{-1/VN(E_F)} \qquad (1.\ 4)$$

if $N(E_F)V \ll 1$. And the BCS reduced hamiltonian is

$$H_{red} = \sum \varepsilon_k (c_k^+ c_k + c_{-k}^+ c_{-k}) - V \sum c_{k'}^+ c_{-k'}^+ c_{-k} c_k \qquad (1.\ 5)$$

which operates only within the pair subspace.

The strong coupling theory was developed by Eliashberg,[14] and this theory is an accurate theory of superconductivity which provides a quantitative explanation of essentially all superconducting phenomena, including the observed deviations from the universal laws of weak-coupling BCS theory. Eliashberg derived a pair of coupled integral equations which relate a complex energy gap function $\Delta(\omega)$ and a complex renormalization parameter $Z_S(\omega)$ for the superconducting state to the electron-phonon and the electron-electron interactions in the normal state. The Eliashberg equations may be quoted at T=0 as (where $\hbar$ is set to 1):

$$\Delta(\omega) = \frac{1}{Z_S(\omega)} \int_0^{\omega_c} d\nu Re\{\frac{\Delta(\nu)}{[\nu^2 - \Delta^2(\nu)]^{-1/2}}\}\{K_+(\nu,\omega) - N(E_F)U_c\} \qquad (1.\ 6)$$

$$[1 - Z_s(\omega)]\omega = \int_0^{\infty} d\nu Re\{\frac{\nu}{[\nu^2 - \Delta^2(\nu)]^{1/2}}\}K_-(\nu,\omega) \qquad (1.\ 7)$$

$$K_{\pm}(\nu,\omega) = \int_0^{\omega_{max}} d\omega' \alpha^2 F(\omega')(\frac{1}{\omega + \omega' - \nu + i\delta} \mp \frac{1}{\omega - \omega' - \nu + i\delta}), \qquad (1.\ 8)$$

where $F(\omega)$ is the phonon density of states.

Some modern treatments of the general microscopic theory of superconductivity are based on the Gor'kov equations.[15] In this approach, a superconductor in an external magnetic field is described by the following set of coupled equations:

$$(i\hbar\omega_n - \hat{H})G(\mathbf{r},\mathbf{r}',\omega_n) + \Delta^*(\mathbf{r})F(\mathbf{r},\mathbf{r}',\omega_n) = \hbar\delta(\mathbf{r} - \mathbf{r}') \qquad (1.\ 9)$$

$$(i\hbar\omega_n + \hat{H}^*)F(\mathbf{r},\mathbf{r}',\omega_n) + \Delta(\mathbf{r})G(\mathbf{r},\mathbf{r}',\omega_n) = 0 \qquad (1.\ 10)$$

In these equations, G and F are the usual temperature dependent Green's functions. For finite temperatures the frequencies $\hbar\omega_n = (2n+1)\pi kT$ guarantee

the proper Fermi statistics. $\hat{H}$ is the full electron Hamiltonian measured from the chemical potential, and includes the interaction of the electrons with boundaries, with impurities, and with the magnetic field. $\hat{H}$ differs from $\hat{H}^*$ by the sign of the magnetic field. The equations of motion above have to be solved together with the self-consistency equation

$$\Delta(\mathbf{r}) = gF(\mathbf{r}, \mathbf{r}) = (gkT/\hbar) \sum_n F(\mathbf{r}, \mathbf{r}, \omega_n) \tag{1. 11}$$

where g is the strength of the attractive delta function.

If we consider a more general case of electron gas with attractive interactions, where the electrons also experience an arbitrary external potential $U_0(\mathbf{r})$, and a magnetic field $H = curl A$, it will be important to describe the impurities in the specimen. Bogoliubov described a method to treat $U_0(\mathbf{r})$, which is essentially a generalization of the Hartree-Fock equations to the case of superconductivity. In short. the Bogoluibov-de Gennes equations may be written as[16]

$$\epsilon u(\mathbf{r}) = [H_e + U_0(\mathbf{r})]u(\mathbf{r}) + \Delta(\mathbf{r})v(\mathbf{r}) \tag{1. 12}$$

$$\epsilon v(\mathbf{r}) = -[H_e^* + U_0(\mathbf{r})]v(\mathbf{r}) + \Delta^*(\mathbf{r})u(\mathbf{r}) \tag{1. 13}$$

where $u(\mathbf{r})$ and $v(\mathbf{r})$ are defined as

$$\psi(\mathbf{r} \uparrow) = \sum_n (\gamma_{n\uparrow} u_n(\mathbf{r}) - \gamma_{n\downarrow}^+ v_n^*(\mathbf{r})) \tag{1. 14}$$

$$\psi(\mathbf{r} \downarrow) = \sum_n (\gamma_{n\downarrow} u_n(\mathbf{r}) + \gamma_{n\uparrow}^+ v_n^*(\mathbf{r})) \tag{1. 15}$$

and the $\psi(r \uparrow)$ and $\psi(r \downarrow)$ are the field operators. $H_e$ and $H_e^*$ are defined as:

$$H_e = \frac{1}{2m}(-i\hbar\nabla - \frac{e\mathbf{A}}{c})^2 + U_0(\mathbf{r}) - E_F \tag{1. 16}$$

$$H_e^* = \frac{1}{2m}(i\hbar\nabla - \frac{e\mathbf{A}}{c})^2 + U_0(\mathbf{r}) - E_F \neq H_e \tag{1. 17}$$

when a magnetic field is present.

## 1.2 Motivation

At first sight, it seems that superconductivity is well understood. However, the discovery of high $T_c$ superconducting oxides[17] casts a doubt on this belief. The

origin of the superconductivity in high $T_c$ cuprates remains puzzling and the conventional theory is not applicable to high $T_c$ superconductors. The electron-phonon interaction is not strong enough to give rise to $T_c$ higher than 100K. On the other hand, even with conventional superconductors there are many unexplained experiments.[18-20] For instance, impurity effects[18,19] and junction problems[20] showed many discrepancies between theory and experiments.

Recently, a possible resolution of the impurity problem was suggested by Kim and Overhauser.[21,22] For a magnetic impurity Kim and Overhauser[22] developed a BCS type theory. In this theory, the magnetic interaction between a conduction electron at r and a magnetic impurity located at $R_i$ is given by

$$H_m(r) = J\mathbf{s} \cdot \mathbf{S}_i v_0 \delta(r - R_i) \qquad (1.\ 18)$$

where the magnetic impurity has spin $\mathbf{S}$, $\mathbf{s} = \frac{1}{2}\sigma$ and $v_0$ is the atomic volume. Including the magnetic interaction, the BCS $T_c$ equation still applies after a modification of the effective coupling constant,

$$\lambda_{eff} = \lambda < \cos\theta >^2 \qquad (1.\ 19)$$

where $\theta$ is the canting angle of the basis pairs. Accordingly, the BCS $T_c$ equation turns out to be

$$k_B T_c = 1.13\hbar\omega_D e^{-\frac{1}{\lambda_{eff}}} \qquad (1.\ 20)$$

and initial slope is given by

$$k_B(\Delta T_c) \cong -\frac{0.63\hbar}{\lambda\tau_s} \qquad (1.\ 21)$$

It is clear from this equation that the initial slope contains a term $1/\lambda$ and depends on the superconductor. Hence it is not a universal constant. When the conduction electrons have a mean free path $\ell$ that is smaller than the coherence length $\xi_0$ (for a pure superconductor) the effective coherence length is defined as $\xi_{eff} \approx \sqrt{\ell\xi_0}$. Also for a superconductor which has ordinary impurities as well as magnetic impurities, total mean free path is given by

$$\frac{1}{\ell} = \frac{1}{\ell_s} + \frac{1}{\ell_0} \qquad (1.\ 22)$$

where $\ell_0$ is the potential scattering mean free path and $\ell_s$ is the mean free path for exchange scattering only. Therefore, the initial slope of the $T_c$ depression is decreased in the following way:

$$k_B(\Delta T_c) \cong -\frac{0.63\hbar}{\lambda \tau_s}\sqrt{\frac{\ell}{\xi_0}}. \qquad (1.\ 23)$$

Ordinary impurities can lead to weak localization and can also have important effects in superconductors.[23] Although the conventional theory based on Anderson's Theorem[24] states that $T_c$ is not influenced by disorder, we can see that superconductivity and localization are competing in one, two and three dimensional systems from the experimental results.[18,19] Kim[23] has studied the effect of weak localization on superconductors within BCS theory, and pointed out that conductivity and phonon-mediated interaction in superconductors have the same correction terms (Table 1.1). It is shown that weak localization decreases the electron-phonon coupling constant, therefore suppressing $T_c$.

| disorder limit | dirty | weak localization | | strong localization |
|---|---|---|---|---|
| conductivity | $\sigma_B$ | $\sigma_B[1 - \frac{2}{\pi k_F \ell}\ln(L/\ell)]$ | (2d) | $\sim \exp(-\alpha L)$ |
| | | $\sigma_B[1 - \frac{3}{(k_F \ell)^2}(1 - (\ell/L))]$ | (3d) | |
| phonon mediated | V | $V[1 - \frac{2}{\pi k_F \ell}\ln(L/\ell)]$ | (2d) | $\sim \exp(-\alpha L)$ |
| interaction | | $V[1 - \frac{3}{(k_F \ell)^2}(1 - (\ell/L))]$ | (3d) | |

Table 1.1: Comparison of conductivity and phonon mediated interaction in dirty, weak localization and strong localization limits. Here $\alpha$ denotes the inverse of localization length

Consequently weak localization has a strong influence on both the phonon-mediated interaction and the electron phonon interaction. At high temperatures, the phonon limited electrical resistivity is given by[25]

$$\rho_{ph}(T) = \frac{4\pi m k_B T}{n e^2 \hbar}\int \frac{\alpha_{tr}^2 F(\omega)}{\omega}d\omega \qquad (1.\ 24)$$

where $\alpha_{tr}$ includes an average of a geometrical factor $1 - \cos\theta_{\mathbf{kk'}}$. Assuming

$\alpha_{tr}^2 \cong \alpha^2$, we obtain

$$\rho_{ph}(T) \cong \frac{2\pi m k_B T}{ne^2 \hbar} \lambda_{eff} \cong \frac{2\pi m k_B T}{ne^2 \hbar} N_0 \frac{I_0^2}{M\omega_D^2}[1 - \frac{3}{(k_F l)^2}] \tag{1. 25}$$

This basically explains the physical origin of the Mooij Rule.[26]

In this thesis, using Kim and Overhauser's theory we investigate magnetic impurity effect in superconductors and weak-localization effect on the electron-phonon interaction.

# Chapter 2

# Magnetic Impurity Effect in Superconductors

It has been observed by the experimentalists that the effect of magnetic impurity on superconductors differs if the host superconductor is in the crystalline state or in the amorphous state.[27-36] For instance, the decrease of the initial slope of $T_c$ due to magnetic impurities does not show a universal behavior, but depends on sample quality and sample preparation methods. This was not well understood. Kim and Overhauser[22] have recently proposed a theory explaining the magnetic impurity effect on superconductors, which reaches agreement with experimental results.[37] The following results were predicted:

(1) The initial decrease of the slope of $T_c$ due to magnetic impurities is not a universal constant as suggested by Abrikosov and Gor'kov,[38] but depends on the superconductor.

(2) The reduction of $T_c$ by magnetic impurities is significantly lessened whenever the mean free path $\ell$ becomes smaller than the BCS coherence length $\xi_0$.

(3) If the host superconductor is pure enough for exchange scattering to dominate, $T_c$ drops suddenly from about 50% of $T_{c0}$ (for the pure metal) to zero near the critical impurity concentration. This may be called the *pure limit behavior*[33] that was first discovered by Roden and Zimmermeyer[32] in crystalline

Cd.

The first result becomes evident, since it is observed that the initial decrease of $T_c$ for superconductors as a function of $c$, the concentration of magnetic ions, is bigger in the crystalline state than that in the amorphous state of superconductors. In Table 2.1, literature data for the initial decrease of $T_c$ for Zn-Mn system are listed. These data confirm this behavior. As can be seen, the initial slope of the decrease of $T_c$ due to magnetic impurities is not universal but dependent on the sample quality and sample preparation methods. This behavior is also related to the mean free path $\ell$. The compensation phenomenon described as the second result has been observed by adding non-magnetic impurities[27,28] and radiation damage.[29,30,34] The *pure limit behavior* is hard to observe experimentally due to the metalurgical problems related to a very small solubility of magnetic impurities in non-transition metals. Also adding many magnetic impurities may result in a disordered host superconductor. Therefore, it is really remarkable that Roden and Zimmermeyer[32] confirmed, the *pure limit behavior* in crystalline Cadmium doped with dilute Mn atoms by quench condensation. Remarkably, they found that a quench-condensed film of cadmium in the microcrystalline state shows an abrupt decrease of the transition temperature near the critical impurity concentration.

| $-(dT_c/dc)_{initial}$ in [K/at %] | sample | Reference |
|---|---|---|
| 170 | bulk | [40] (1964) |
| 315 | bulk | [28] (1966) |
| >300 | bulk | [41] (1968) |
| 260 (290) | bulk | [42] (1971) |
| 300 | bulk | [43] (1972) |
| 630 | single crystal | [33] (1975) |
| 215 | thin film | [44] (1967) |
| 285 | thin film | [39] (1967) |

Table 2.1: Values for the initial depression $-(dT_c/dc)_{initial}$ of the $T_c$ of Zn with different concentrations of Mn. Data are from Falke et al., Ref. 39.

In this chapter, in section 2.1 a brief review of experimental studies is given, in section 2.2 KO (Kim-Overhauser) theory is described, in section 2.3 comparison

with various experimental data is given and in section 2.4 the implication of this study is given briefly.

## 2.1 Magnetic Impurity Effect in Crystalline and Amorphous States of Superconductors

In this Section, experimental data for the effect of magnetic impurities in crystalline and amorphous states of superconductors are briefly reviewed. Although there are already a few review articles on magnetic impurity effect in superconductors,[48,49] this topic was not spotlighted before, simply because the experimental data were not understood. Nevertheless, it was observed by many experimentalists that the magnetic impurity effects are different for crystalline and amorphous states of superconductors. To illustrate, the initial decrease of $T_c$ for some superconductors as a function of the concentration c of the magnetic ions are summarized in Table 2.2. The Table is from Buckel,[36] Wassermann,[29] and Schwidtal.[59] It is clear that the initial $T_c$ decrease depends on the sample quality. Note that In-Mn,[30,31,34] Sn-Mn,[53] Zn-Mn,[39] and Cd-Mn[60] show the Kondo anomalies at low temperatures.

Merriam, Liu, and Seraphim[27] were the first who found the difference. They investigated the effect of dissolved Mn on superconductivity of pure and impure In. They observed that the addition of a third element, Pb or Sn, progressively decreases the effect of Mn and eliminates the effect completely when the mean free path is decreased sufficiently enough. In other words, the $T_c$ depression arising from a paramagnetic solute turned out to be mean-free-path dependent. Boato, Gallinaro, and Rizzuto[28] confirmed the result. It was also found that $T_c$ depression by transition metal impurities in bulk metals and thin films leads very often to different results.[29] For instance, broad scattering of the experimental $-dT_c/dc$ values was frequently obtained, presumably due to the differences in the degree of disorder. A review was given by Wassermann.[29] On the other hand, Falke et al.[39] investigated transition temperature depression in quench

| Superconductor | Additive | | | $-dT_c/dc$ in K/atom % | |
|---|---|---|---|---|---|
| Pb | Mn | | | 21* (a), | 16** (b) |
| Sn | Mn | | | 69* (c), | 14** (b) |
| Zn | Mn | 315 (d), | 285* (e), | 343** (f), | 630 (g) |
| Zn | Cr | | | 170 (d), | 90-200 (h) |
| Cd | Mn | | | 44 (i), | 5.4* (j) |
| In | Mn | 25 (k), | 53* (l), | 50** (m), | 100 (n) |
| In | Fe | | | 2.5 (l), | 2.0 (o) |
| La | Gd | | | 5.1* (p), | 4.5** (q) |

Table 2.2: Reduction in the $T_c$ of some superconductors by magnetic impurities. Data are from Buckel, Ref. 36, Wassermann, Ref. 29, and Schwidtal, Ref. 51. * quench-condensed films ** ion implantation at low temperatures. References: a):[52]; b):[53]; c):[54]; d):[28]; e):[39]; f):[55]; g):[33]; h):[29]; i):[44]; j):[32]; k):[30]; l):[55]; m):[34]; n):[27]; o):[57]; p):[58]; q):[59]

condensed Zn-Mn dilute alloy films and compared it with bulk data. Their work gives good support to the equivalence of thin films and bulk material. To put it another way, even though the initial $T_c$ depression caused by magnetic impurities may be different for thin films and bulk material, a magnetic impurity may possess a stable magnetic moment whether it is in thin films or in bulk material. Bauriedl and Heim[30] noted that the reason for the different behavior of magnetic impurities in crystalline and disordered materials is lattice disorder. The authors considered annealed In films implanted with 150 keV-Mn ions at low temperatures and increased the lattice disorder by pre-implantation of In ions, which led to variations of the initial $T_c$-depression between 26 K/at % for the crystalline sample and 10 K/at % for the heavily disordered sample. Hitzfeld and Heim[31] reported that the magnetic state of Mn in ion implanted In-Mn alloys is not so much affected by incorporating oxygen (lattice disorder) but that the superconducting properties change significantly, in agreement with Falke et al.[39]: $-dT_c/dc$ is changed from 24 to 18 K/at % if oxygen is added. Schlabitz and Zaplinski[33] reported on the influence of lattice defects on the $T_c$-depression in dilute Zn-Mn single crystals. Their measurements also show a much

higher depression of $T_c$ for single crystals than for cold-rolled crystals and quench-condensed films. Hofmann, Bauriedl, and Ziemann[34] also observed compensation of the effect of paramagnetic impurities as a consequence of radiation damage. Well annealed In-films implanted at low temperatures with Mn ions lead to an initial slope of 50 K/at %, whereas In-films irradiated with high fluences of Ar ions before the Mn-implantation lead to a slope of 39 K/at %. In addition, 90% of the 2.2 K decrease in $T_c$ caused by Mn-implantation was suppressed by an Ar fluence of $2.2 \times 10^{16} cm^{-2}$. Habisreuther et al.[35] reported on an *in situ* low-temperature ion-implantation study of Mn in crystalline $\beta$-Ga and amorphous $a$-Ga films. They found linear $T_c$ decreases in $a-$Ga films with a slope of 3.4 K/at % and in $\beta-$Ga films with a slope of 7.0 K/at %, (i.e., twice as large as in $a-$Ga).

Furthermore, Roden and Zimmermeyer[32] considered crystalline and amorphous cadmium with dilute Mn atoms. In the first case the initial depression of $T_c$ is $-dT_c/dc=5.4$ K/at % and in the second case it is $-dT_c/dc=2.65$ K/at % in accordance with other results. Surprisingly, a sudden drop of $T_c$ in crystalline cadmium near the critical concentration was observed. About 50 % of $T_{c0}$ was decreased to zero by adding additional tiny amounts of Mn atoms in the (micro)crystalline state, which has been predicted by Kim and Overhauser. Since the transition temperature of pure Cd in the crystalline state is 0.9 K ($T_{c0}$), the critical Mn impurity concentration is so low ($\sim$ 0.075 at %) that the crystalline state is not much disturbed by Mn atoms. Consequently, the *pure limit behavior* of magnetic impurity effect was observable. Zimmermeyer and Roden[61] also found similar behavior in microcrystalline films of lead doped with Mn, but with a peak just before $T_c$ drops to zero suddenly. The critical concentration is $\sim$ 0.4 at %. In this case, since the initial $T_c$ depression is not linear as a function of Mn concentration, there seems to be some solubility problem.

## 2.2 Theory of Kim and Overhauser

### 2.2.1 Ground State Wavefunction

For a homogeneous system, the BCS wavefunction is given by[13,62]

$$\tilde{\phi} = \prod_k (u_k + v_k a_{k\uparrow}^\dagger a_{-k\downarrow}^\dagger)\phi_0 \tag{2. 1}$$

where the operator $a_{k\alpha}^\dagger$ creates an electron in the state $(k\alpha)$ (with the energy $\epsilon_k$) when operating on the vacuum state designated by $\phi_0$. Note that $\tilde{\phi}$ is an approximation of $\phi_N$,

$$\phi_N = A[\phi(r_1 - r_2) \cdots \phi(r_{N-1} - r_N)(1 \uparrow)(2 \downarrow) \cdots (N-1 \uparrow)(N \downarrow)] \tag{2. 2}$$

where

$$\phi(r) = \sum_k \frac{v_k}{u_k} e^{i\mathbf{k}\cdot\mathbf{r}} \tag{2. 3}$$

and both wavefunctions lead to the same result for a large system. Nevertheless, $\phi_N$ is more helpful for understanding the underlying physics related to the magnetic impurity effect in superconductors: we are concerned with a bound state of Cooper pairs in a BCS condensate. It should be noticed that the (bounded) pair wavefunction $\phi(r)$ and the BCS pair-correlation amplitude $I(r)$[13] are basically the same for large N:

$$\phi(r) = \sum_k \frac{\Delta_k}{\epsilon_k + E_k} e^{i\mathbf{k}\cdot\mathbf{r}}, \tag{2. 4}$$

$$I(r) = \sum_k \frac{\Delta_k}{2E_k} e^{i\mathbf{k}\cdot\mathbf{r}} \sim \Delta K_0(\frac{r}{\pi\xi_0}), \tag{2. 5}$$

where

$$E_k = \sqrt{\epsilon_k^2 + \Delta_k^2}. \tag{2. 6}$$

Here $K_0$ is a modified Bessel function which decays rapidly when $r > \pi\xi_0$.

In the presence of magnetic impurities, BCS pairing must employ degenerate partners which have the exchange scattering (due to magnetic impurities) built in because the strength of exchange scattering $J$ is much larger than the binding energy. This scattered state representation was first introduced

by Anderson[24] in his theory of dirty superconductors. Accordingly, the corresponding wavefunctions are

$$\tilde{\phi}' = \prod_n (u_n + v_n a_{n\uparrow}^\dagger a_{\bar{n}\downarrow}^\dagger)\phi_0 \tag{2. 7}$$

and

$$\phi_N' = A[\phi'(r_1, r_2)\phi'(r_3, r_4) \cdots \phi'(r_{N-1}, r_N)] \tag{2. 8}$$

where

$$\phi'(r_1, r_2) = \sum_n \frac{v_n}{u_n} \psi_{n\uparrow}(r_1)\psi_{\bar{n}\downarrow}(r_2). \tag{2. 9}$$

Here $\psi_n$ and $\psi_{\bar{n}}$ denote the exact eigenstate and its degenerate partner, respectively. It is clear from the pair wavefunction $\phi'(r_1, r_2)$ that only the magnetic impurities within $\xi_0$ of a Cooper pair's center of mass can diminish the pairing interaction.

## 2.2.2 Phonon-mediated matrix element

Now we need to determine the scattered state $\psi_n$ and the phonon-mediated matrix element $V_{nn'}$. The magnetic interaction between a conduction electron at **r** and a magnetic impurity (having spin **S**), located at $\mathbf{R}_i$, is given by

$$H_m(\mathbf{r}) = J\mathbf{s} \cdot \mathbf{S}_i v_o \delta(\mathbf{r} - \mathbf{R}_i), \tag{2. 10}$$

where $\mathbf{s} = \frac{1}{2}\sigma$ and $v_o$ is the atomic volume. The scattered basis state which carries the label, $n\alpha = \vec{k}\alpha$, is then

$$\psi_{n=\vec{k}\alpha} = N_{\vec{k}}[e^{i\vec{k}\cdot\vec{r}}\alpha + \sum_{\vec{q}} e^{i(\vec{k}+\vec{q})\cdot\vec{r}}(W_{\vec{k}\vec{q}}\beta + W_{\vec{k}\vec{q}}'\alpha)], \tag{2. 11}$$

where,

$$W_{\vec{k}\vec{q}} = \frac{\frac{1}{2}J\bar{S}v_o}{\epsilon_{\vec{k}} - \epsilon_{\vec{k}+\vec{q}}} \sum_j sin\chi_j e^{i\phi_j - i\vec{q}\cdot\mathbf{R}_j} \tag{2. 12}$$

and,

$$W_{\vec{k}\vec{q}}' = \frac{\frac{1}{2}J\bar{S}v_o}{\epsilon_{\vec{k}} - \epsilon_{\vec{k}+\vec{q}}} \sum_j cos\chi_j e^{-i\vec{q}\cdot\mathbf{R}_j}. \tag{2. 13}$$

$\chi_j$ and $\phi_j$ are the polar and azimuthal angles of the spin $\mathbf{S}_j$ at $\mathbf{R}_j$ and $\overline{S} = \sqrt{S(S+1)}$. The perturbed basis state for the degenerate partner of (2.11) is:

$$\psi_{\hbar\beta=-\vec{k}\beta} = N_{\vec{k}}[e^{-i\vec{k}\cdot\vec{r}}\beta + \sum_{\vec{q}} e^{-i(\vec{k}+\vec{q})\cdot\vec{r}}(W_{\vec{k}\vec{q}}^* \alpha - W_{\vec{k}\vec{q}'}'^* \beta)]. \qquad (2.\ 14)$$

At each point $\vec{r}$, the two spins of the degenerate partner become canted by the mixing of the plane wave and spherical-wavelet component. Consequently, the BCS condensate is forced to have a triplet component because of the canting caused by the exchange scattering. The phonon-mediated matrix element between the canted basis pairs is (to order $J^2$)

$$V_{nn'} = V_{\vec{k}'\vec{k}} = -V < cos\theta_{\vec{k}'}(\vec{r}) >< cos\theta_{\vec{k}}(\vec{r}) >, \qquad (2.\ 15)$$

where $\theta$ is the canting angle. The angular brackets indicate both a spatial and impurity average. It is then given

$$< cos\theta_{\vec{k}}(\vec{r}) > \cong 1 - 2|W_{\vec{k}}|^2, \qquad (2.\ 16)$$

where $|W_{\vec{k}}|^2$ is the relative probability contained in the virtual spherical waves surrounding the magnetic solutes (compared to the plane-wave part). From Eqs. (2.11)-(2.13) we obtain

$$|W_{\vec{k}}|^2 = \frac{J^2 m^2 \bar{S}^2 c_m R}{8\pi n \hbar^4}. \qquad (2.\ 17)$$

Because the pair-correlation amplitude falls exponentially as $exp(-r/\pi\xi_o)^{13}$ at $T = 0$ and as $exp(-r/3.5\xi_o)^{63}$ near $T_c$, we set

$$R = \frac{3.5}{2}\xi_o. \qquad (2.\ 18)$$

Then one finds

$$< cos\theta >= 1 - \frac{3.5\xi_o}{2\ell_s}, \qquad (2.\ 19)$$

where $\ell_s = v_F \tau_s$ is the mean free path for exchange scattering only.

## 2.2.3   BCS $T_c$ equation

The resulting BCS gap equation, near $T_c$, is given by

$$\overline{\Delta_{\vec{k}}} = -\sum_{\vec{k}'} \overline{V_{\vec{k},\vec{k}'}} \frac{\overline{\Delta_{\vec{k}'}}}{2\overline{\epsilon_{\vec{k}'}}} tanh(\frac{\overline{\epsilon_{\vec{k}'}}}{2T}). \qquad (2.\ 20)$$

Here $\overline{\Delta_{\vec{k}}}$ is the impurity averaged values of the gap parameter whereas $\overline{\epsilon_{\vec{k}}}$ is that of the electron energy. The BCS $T_c$ equation still applies after a modification of the effective coupling constant according to Eq. (2.15):

$$\lambda_{eff} = \lambda < cos\theta >^2, \qquad (2.\ 21)$$

where $\lambda$ is $N_oV$. Accordingly, the BCS $T_c$ equation is now,

$$k_BT_c = 1.13\hbar\omega_De^{-\frac{1}{\lambda_{eff}}}. \qquad (2.\ 22)$$

The initial slope is given

$$k_B(\Delta T_c) \cong -\frac{0.63\hbar}{\lambda\tau_s}. \qquad (2.\ 23)$$

The factor $1/\lambda$ shows that the initial slope depends on the superconductor and is not a universal constant. For an extended range of solute concentration, KO find

$$< cos\theta >= \frac{1}{2} + \frac{1}{2}[1 + 5(\frac{u}{2})^2]^{-1}e^{-2u}, \qquad (2.\ 24)$$

where

$$u \equiv 3.5\xi_{eff}/2\ell_s. \qquad (2.\ 25)$$

## 2.2.4   Change of the initial slope of the $T_c$ decrease

When the conduction electrons have a mean free path $\ell$ which is smaller than the coherence length $\xi_o$ (for a pure superconductor), the effective coherence length is

$$\xi_{eff} \approx \sqrt{\ell\xi_o}. \qquad (2.\ 26)$$

For a superconductor which has ordinary impurities as well as magnetic impurities, the total mean-free path $\ell$ is given by

$$\frac{1}{\ell} = \frac{1}{\ell_s} + \frac{1}{\ell_o}, \qquad (2.\ 27)$$

where $\ell_o$ is the potential scattering mean free path. It is evident from Eq. (2.26) that the potential scattering profoundly affects the paramagnetic impurity effect.

Consequently, the initial slope of the $T_c$ depression is decreased in the following way:

$$k_B(\Delta T_c) \cong -\frac{0.63\hbar}{\lambda \tau_s}\sqrt{\frac{\ell}{\xi_0}}. \qquad (2.\ 28)$$

This explains the broad scattering of the experimental $-dT_c/dc$ values. In other words, the size of the Cooper pair is reduced by the potential scattering and the reduced Cooper pair sees a smaller number of magnetic impurities. Accordingly the magnetic impurity effect is partially suppressed, leading to the decrease of the initial slope of the $T_c$ depression.
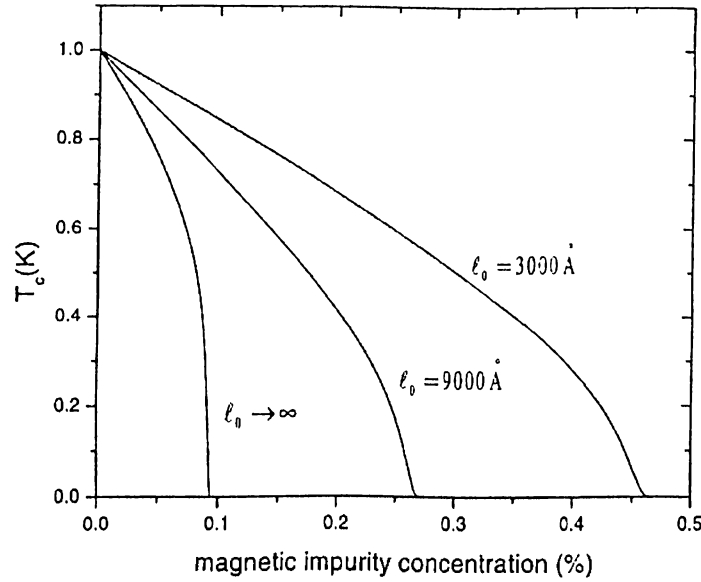


Figure 2. 1: Variation of $T_c$ with magnetic impurity concentration for pure and impure superconductors. $\ell_0$ denotes the mean free path for the potential scattering.

Figure 2.1 shows the different behavior of the $T_c$ depression due to magnetic impurities in the pure crystalline state and in the amorphous or disordered state of superconductors. We used $T_{co} = 1.0K$, $v_F = 1.5 \times 10^8 cm/sec$, and $\omega_D = 250K$. We also assumed the relation between $\ell_s$ and magnetic impurity concentration c: $\ell_s = 10^5/c(\mathring{A})$. Here c is measured in at %. Since the exchange scattering cross-section is usually 20-200 times smaller than that for the potential scattering,[22] this assumption seems to be reasonable. For the pure crystalline state, $T_c$ drops

to zero suddenly when $T_c$ is decreased to about 50 % of $T_{c0}$ of the pure system, which may be called *pure limit behavior*. As the mean free path $\ell$ is decreased due to disorder, the initial $T_c$ depression is weakened and $T_c$ drops to zero more slowly near the critical concentration.

## 2.3    Comparison with Experiment

The overall agreement between KO theory and the existing experimental data is impressive. We focus on the experiments which investigated the difference of the magnetic impurity effect in pure crystalline state and amorphous or disordered state of superconductors.

### 2.3.1   *Pure limit behavior*:    Roden and Zimmermeyer's Experiment

Roden and Zimmermeyer[32] prepared alloys of Cd with dilute Mn impurities by quench condensation. Quench condensation produces a variety of states of the alloy: in particular, one can get a microcrystalline and an amorphous state. A quench-condensed film of Cd in the microcrystalline state shows a higher $T_c$ (= $0.9K$) than the bulk material and a further increase of $T_c$ (= $1.15K$) is obtained in the amorphous state. Amorphous Cd film was obtained by adding Cu atoms. Like other nontransition metals deposited in an ordinary high-vacuum system, the quench-condensed Cd film is crystalline with small crystallites.[64]

Now we compare KO theory with Roden and Zimmermeyer's experiment. Figure 2.2 shows $T_c$ versus magnetic impurity concentration c in the microcrystalline CdMn. The solid line is the theoretical curve obtained from Eq. (2.22). The transition temperature $T_{c0}$ of pure Cd in this state is 0.9K. While the initial depression of $T_c$ is linear in c with a value of $-dT_c/dc = 5.4K/at\%$, above 0.05% the depression becomes much more stronger than linear, which agrees with KO theory. Arrows denote that no superconductivity was found up to 70mK. For theoretical fitting we used $T_{c0} = 0.904K$, $\omega_D = 209K$, and

$v_F = 1.62 \times 10^8 cm/sec.$[65] We emphasize that there is no free parameter. In the absence of experimental data we assumed $\ell_s = 9 \times 10^5/c(\mathring{A})$. As can be seen, the agreement between the experimental data and the theoretical curve is very good.
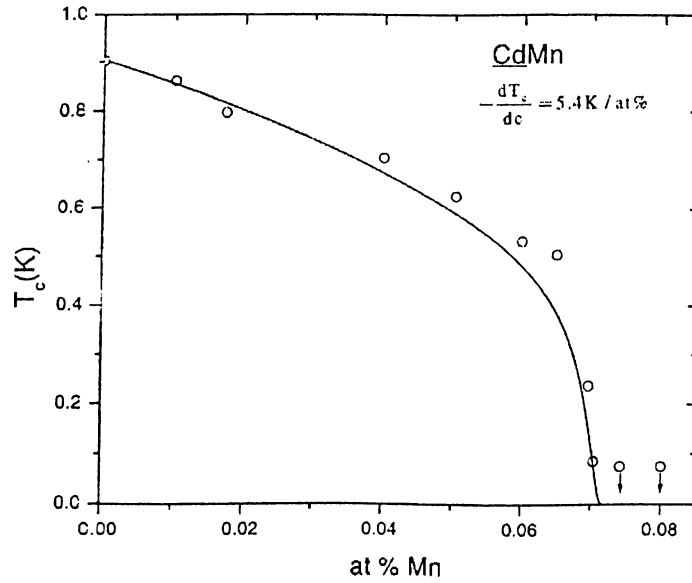


Figure 2.   2:  Comparison of the experimental data for CdMn in the microcrystalline state with the KO theory. Experimental data are from Roden and Zimmermeyer, Ref. 32

Figure 2.3 shows $T_c$ vs. c for the amorphous CdCuMn. The solid line was obtained from Eqs. (2.22) and (2.26). The decrease of $T_c$ for smaller c is again linear but with a much lower $-dT_c/dc = 2.65 K/at\%$. In the amorphous state $T_{c0}$ is about 1.18K. Since the residual resistivity data are not available, we assumed that the mean free path for the potential scattering is $\ell_o = 4500\mathring{A}$ which is reasonable. We used the same values for $\omega_D$ and $v_F$ as in Fig. 2.2. Again we find a good fitting to experimental data.
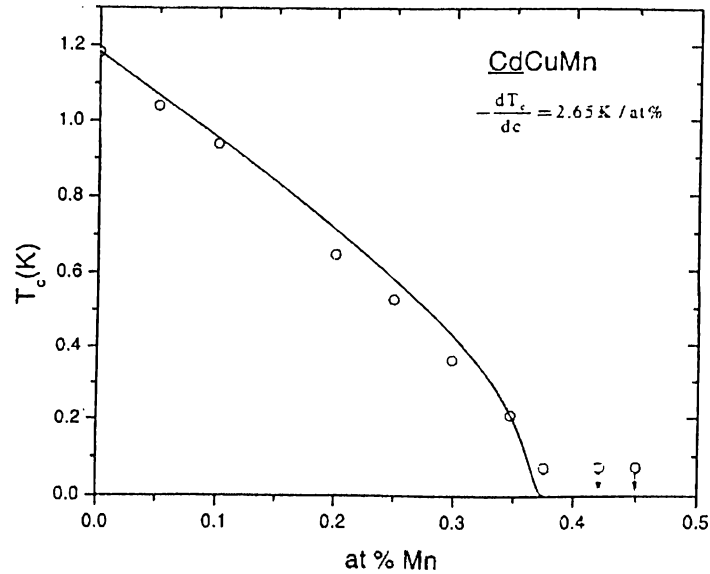
Figure 2. 3: Comparison of the experimental data for CdMn in the amorphous state with the KO theory. Experimental data are from Roden and Zimmermeyer, Ref. 32

## 2.3.2 Change of the initial slope of the $T_c$ depression

Schlabitz and Zaplinski[33] reported measurements of the $T_c$-depression of ZnMn single crystals. In particular, they investigated the influence of lattice defects on the $T_c$-depression in dilute ZnMn single crystals. They demonstrated linear behavior up to a concentration of 10 ppm with a slope of 630 K/at%. This value is twice that of other measurements. As a result, they suggested that the $T_c$-depression can be enhanced strongly by eliminating the lattice defects.

Figure 2.4 shows the reduced transition temperature, $T_c/T_{c0}$, as a function of Mn concentration. The dashed lines, taken from the other measurements,[39] give the $T_c$-depression of: a) quench-condensed films, and b) cold rolled bulk material. The filled points represent the $T_c$-values of the ZnMn single crystals. The filled squares are the data of quench condensed thin films, while the filled triangles are the data of quench condensed thin films after annealing at $300K$ for 14 hours. Since annealing leads to an increased order of the lattice,[64] it is clear that the initial slope of the $T_c$ decrease is decreasing as the system is getting disordered.
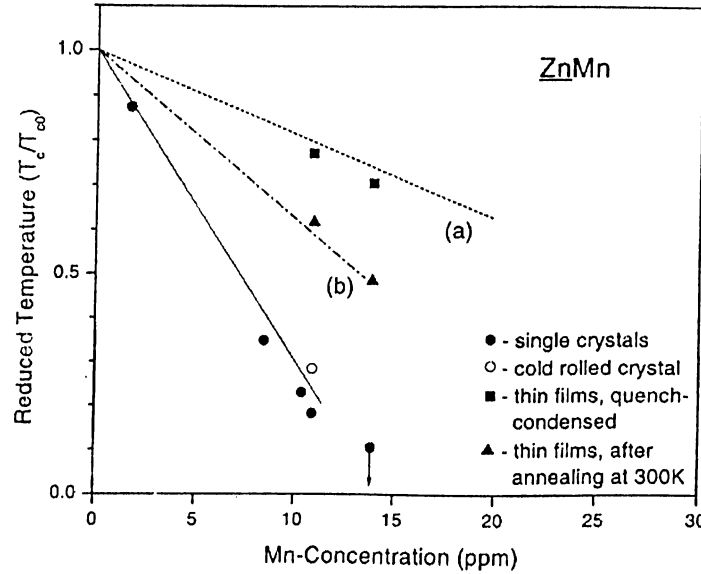
Figure 2. 4: Reduced transition temperature versus Mn concentration for ZnMn. The solid line is the theoretical curve obtained from Eq. (2.29). Line (a): Data of thin films from Ref. 39, line (b): Data of cold rolled bulk material from Refs 28 and 42. Data are from Schlabitz and Zaplinski, Ref. 33.

The solid line is the theoretical curve obtained from the initial slope, $-dT_c/dc = 630K/at\%$ with $T_{c0} = 0.9K$:

$$k_B T_c \cong k_B T_{c0} - \frac{0.63\hbar}{\lambda \tau_s}. \qquad (2.\ 29)$$

This expression agrees very well with the exact BCS $T_c$ equation, Eq. (2.22), up to 25 % of the critical impurity concentration. The dashed lines (a) and (b) can also be reproduced from the theoretical formula, Eq. (2.28), for the initial $T_c$ depression in the disordered state of superconductors with $(a)$ : $\ell = 7520\mathring{A}, T_{c0} = 0.83K,$[39] and $(b)$ : $\ell = 3390\mathring{A}, T_{c0} = 1.51K,$[39] respectively. Here $T_{c0}$ values are the experimental results.[39] Therefore, the change of the initial slope of the $T_c$ decrease may be explained in terms of the change of the Cooper pair size caused by the variation of the mean free path $\ell$. We used $\omega_D = 327K$, and $v_F = 1.82 \times 10^8 cm/sec.$[65] The sudden drop of $T_c$ near the critical concentration is not pronounced though, presumably because of the smallness of the critical concentration. Since there are not many magnetic impurities in the Zn

matrix, the distribution of Mn may be atomically disperse but macroscopically inhomogeneous. Then, the *pure limit behavior* may not be observable.

Bauriedl and Heim[30] investigated the influence of lattice disorder on the magnetic properties of InMn alloys. Crystalline In films were implanted by Mn ions. The amount of lattice disorder was changed in a very controlled way by pre-implantation of indium with its own ions, which was very effective in producing disordered films.
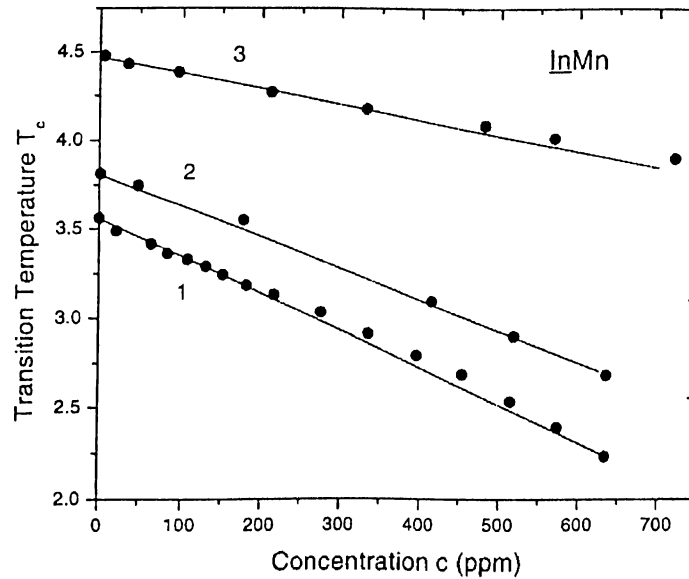


Figure 2. 5: Calculated transition temperatures for implanted InMn alloys. Increasing lattice disorder from 1 to 3 has been produced by pre-implantation of In ions: 1 0ppm, 2 2660ppm, 3 18710ppm. Data are from Bauriedl and Heim, Ref. 30.

Figure 2.5 shows the transition temperatures for InMn alloys with increasing lattice disorder from 1 to 3 by pre-implantation of $In^+$ ions: 1 0ppm; 2 2660ppm; 3 18,710ppm. These ions have an intensive damaging effect, resulting in an increased residual resistivity and an enhanced transition temperature $T_{c0}$.[31] Notice that the initial slope decreases as the system is more disordered. The solid lines are the theoretical results from Eq. (2.28) with $1 : \ell = 1050 \text{Å}$, $2 : \ell = 700 \text{Å}$ and $3 : \ell = 150 \text{Å}$. It is necessary to emphasize that the change of the initial slope due to the enhanced $T_{c0}$ (Eq. (2.23)) is not enough to explain the experimental

data. We assumed the initial slope $-dT_c/dc = 53K/at\%$ for a pure system.[56] We also used $\omega_D = 108K$ and $v_F = 1.74 \times 10^8$.[65] We find good agreements between theory and experiment.

Finally, Habisreuther et al.[35] investigated the magnetic behavior of Mn in crystalline $\beta$−Ga and amorphous $a$−Ga films. Mn ions were implanted at low temperature $(T < 10K)$. The amorphous $a$−Ga exhibits a rather high transition temperature with typical values between 8.1 and 8.4 K, while the crystalline $\beta$−Ga phase shows transition temperature of $T_c = 6.3K$.
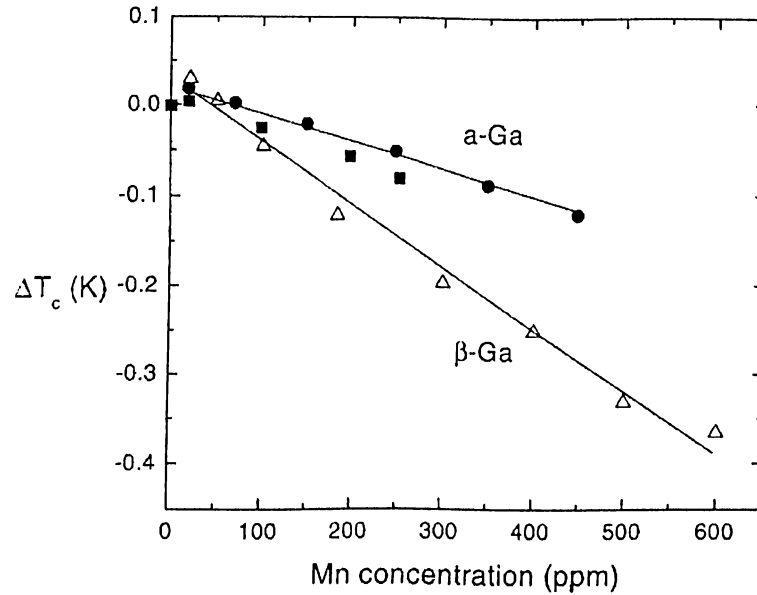


Figure 2. 6: Calculated changes of the superconducting transition temperature $\Delta T_c$ versus impurity concentration for Mn-implanted amorphous $a$−Ga and crystalline $\beta$−Ga. Data are from Habisreuther et al., Ref. 38

Figure 2.6 shows changes of the superconducting transition temperature $\Delta T_c$ produced by Mn implantation into amorphous $a$−Ga films and crystalline $\beta$−Ga films as a function of the impurity concentrations. Note that the initial slope 3.4 K/at % in amorphous $a$−Ga is about half of that (7.0 K/at %) in crystalline $\beta$−Ga films. Theoretical curves represent the initial slope formulas, Eq. (2.23) and (2.28) with $-dT_c/dc = 7K/at\%$, $\ell = \infty$ for $\beta$− Ga, and with $-dT_c/dc = 7K/at\%$, $\ell = 600\text{Å}$ for $a$−Ga. We used $\omega_D = 320K$ and $v_F = 1.91 \times 10^8 cm/sec$.[65]

A good fitting to the experimental data is obtained.

## 2.4 Discussion

It is clear that a systematic experimental study of the effect of magnetic impurities in crystalline and amorphous superconductors is necessary. In particular, the *pure limit behavior* in the crystalline state of superconductors and the change of the initial slope due to disordering need more careful studies. Such investigations may shed a new light on the old question of whether a transition metal impurity possesses a stable local magnetic moment within a metallic host.

The observed *pure limit behavior* in the superfluid He-3 in aerogel may be compared with that in crystalline superconductors including Cd. In superfluid He-3 aerogel does not disturb the liquid state of Helium significantly, whereas in superconductors adding magnetic impurities may damage the crystalline state of the superconductors, resulting in the difficulty in observing the *pure limit behavior*.

In the theoretical fitting we guessed the mean free path $\ell$ because experimental residual resistivity data were not available. If the residual resistivity is given, the mean free path $\ell$ can be determined from the Drude formula. It is interesting to note that the initial $T_c$ depression also provides a way to estimate the mean free path $\ell$.

In this study, weak-coupling BCS theory is used to investigate the effect of magnetic impurities in superconductors. It is straightforward to extend this study to the strong-coupling theory.[14,66] To do that, pairing of the degenerate scattered state partners is also needed.[23] The result will then basically be the same as that of the weak-coupling theory.

# Chapter 3

# Mooij Rule

Although weak localization has greatly deepened our understanding of the normal state of disordered metals,[67,68,69] its effect on superconductivity and the electron-phonon interaction is not well understood.[68] Recently, it was shown that weak localization leads to the same correction to the Boltzman conductivity as to the phonon-mediated interaction.[70,71] In fact, there is an overwhelming number of experiments that support this idea.[71] For instance, tunneling,[72,73,18] specific heat,[74] x-ray photoemission spectra (XPS),[75] correlation of $T_c$ and the residual resistivity,[76-78] universal correlation of the resistance ratio and $T_c$,[79-81] and loss of the thermal resistivity[82] with decreasing $T_c$ clearly show a decrease of the electron-phonon interaction accompanying the decrease of $T_c$ with disorder. It is then anticipated that the electron-phonon interaction in the normal state of metals will also be influenced strongly by weak localization. We expect that phonon-limited electrical resistance, attenuation of a sound wave, thermal resistance, and a shift in phonon frequencies may change due to weak localization.[83]

In early seventies, Mooij found a correlation between the residual resistivity and the temperature coefficient of resistivity (TCR). In particular, TCR is decreasing with increasing the residual resistivity. Then it becomes negative for resistivities above $150\mu\Omega cm$. Indeed, the Mooij rule[26] in strongly disordered metallic systems seems to be a manifestation of the effect of weak localization on the electron-phonon interaction and the conductivity. There are already

several theoretical investigations of this problem. Jonson and Girvin[84] performed numerical calculations for an Anderson model on a Cayley tree and found that the adiabatic phonon approximation breaks down in the high-resistivity regime producing the negative TCR. Imry[85] pointed out the importance of incipient Anderson localization (weak localization) for the resistivities of highly disordered metals. He argued that if the inelastic mean free path, $\ell_{ph}$, is smaller than the coherence length, $\xi$, the conductivity increases with temperature like $\ell_{ph}^{-1}$ and thereby leads to the negative TCR. On the other hand, Kaveh and Mott[86] generalized the Mooij rule. Their results are as follows: The temperature dependence of the conductivity of a disordered metal as a function of temperature changes slope due to weak localization effects, and if interaction effects are included, the conductivity changes its slope three times. Götze, Belitz, and Schirmacher[87,88] introduced a theory with phonon-induced tunneling. There is also the extended Ziman theory,[89] and Jayannavar and Kumar[90] suggested that the Mooij rule can arise from strong electron-phonon interaction taking into account qualitatively different roles of the diagonal and off-diagonal modulations.

In this chapter, we propose an explanation of the Mooij rule based on the effect of weak localization on the electron-phonon interaction. If we assume the decrease of the electron-phonon interaction due to weak localization,[70,71] we can understand the decrease of TCR with increasing the residual resistivity. The negative TCR is therefore due to the weak localization correction to the Boltzmann conductivity, since if TCR is approaching zero, there is no temperature-dependent resistivity left. (This latter point is similar to Kaveh and Mott's interpretation.[86]) In Sec. 3.1, the Mooij rule is briefly described. In Sec. 3.2, weak localization correction to the McMillan's electron-phonon coupling constant $\lambda$ and $\lambda_{tr}$ is calculated. A possible explanation of the Mooij rule is given in Sec. 3.3, and its implication is briefly discussed in Sec. 3.4. In particular, this study may provide a means to probe the phonon-mechanism in exotic superconductors.

## 3.1   The Mooij Rule

Mooij[26] was the first to point out that the size and sign of the temperature coefficient of resistivity (TCR) in many disordered systems correlate with its residual resistivity $\rho_0$ as follows:

$$dp/dT \; > \; 0 \quad \text{if} \quad \rho_0 < \rho_\text{M}$$
$$dp/dT \; < \; 0 \quad \text{if} \quad \rho_0 > \rho_\text{M}. \qquad (3.\; 1)$$

Thus, TCR changes sign when $\rho_0$ reaches the Mooij resistivity $\rho_M \cong 150\mu\Omega cm$. An approximate equation for $\rho(T)$ is given by[68]

$$\rho(T) = \rho_0 + (\rho_M - \rho_0)AT, \qquad (3.\; 2)$$

where $A$ is a constant which depends on the material.
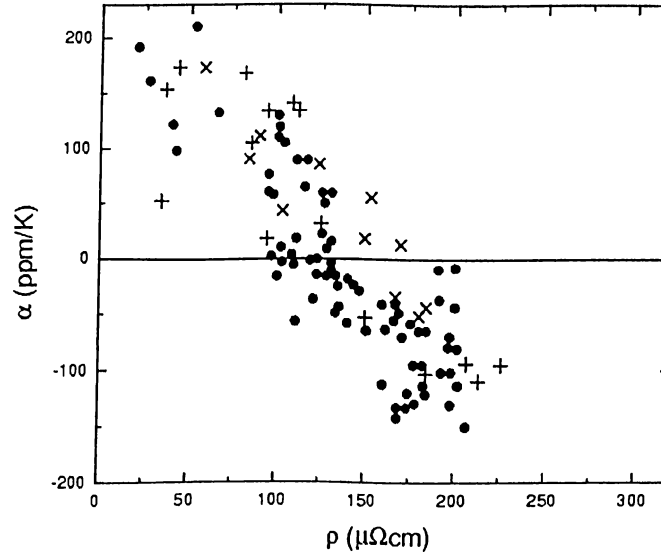


Figure 3. 1: The temperature coefficient of resistance $\alpha$ versus resistivity for bulk alloys (+), thin films ($\bullet$), and amorphous (X) alloys. Data are from Mooij, Ref. 26

Figure 3.1 shows the temperature coefficient of resistance $\alpha$ versus residual resistivity for transition-metal alloys obtained by Mooij. It is clear that $\alpha$ (and

TCR) is correlated with the residual resistivity. Note that above $150\mu\Omega cm$ most $\alpha$'s are negative while no negative $\alpha$ is found for resistivities below $100\mu\Omega cm$. Figure 3.2 shows the resistivity as a function of temperature for pure Ti and TiAl alloys containing 3, 6, 11, and 33% Al. TCR is decreasing as the residual resistivity is increasing. For TiAl alloy with 33% Al shows a negative TCR. We note that positive TCRs are basically high temperature phenomena, presumably related to the phonon-limited resistivity, whereas negative TCRs occurs at low temperature and is probably connected with the residual resistivity. This behavior is generally found in strongly disordered metals and alloys, amorphous metals, and metallic glasses,[68] and is called the Mooij rule. However, the physical origin of this rule has remained unexplained until now.
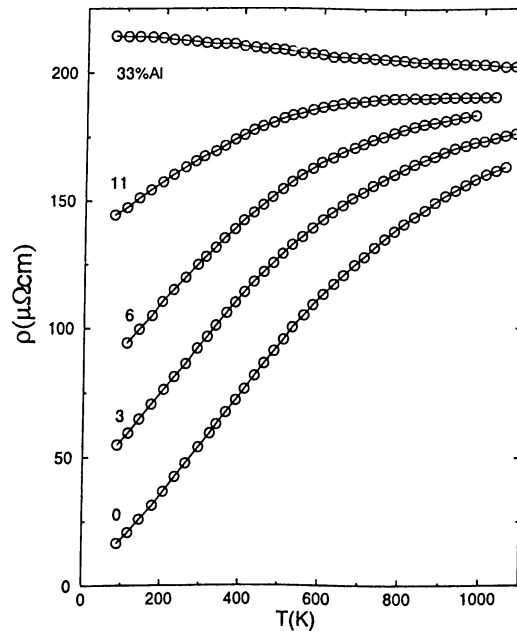


Figure 3. 2: Resistivity versus temperature for Ti and TiAl alloys containing 0, 3, 6, 11, and 33% Al. Data are from Mooij, Ref. 26

# 3.2 Weak Localization Correction to The Electron-Phonon Interaction

Since the electron-phonon interactions in metals give rise to both (high temperature) resistivity and superconductivity, these properties are closely related, as was noticed by many workers.[91-95] Gladstone, Jensen, and Schrieffer[91] pointed out that $\lambda$ and the high temperature electrical resistivity are closely related to each other. Hopfield[92,93] noted that the electronic relaxation time due to electron-phonon interactions, as measured in optical experiments above the Debye temperature, should be approximately equal to $2\pi\lambda k_B T/\hbar$. He applied this idea to Nb, Mo, Al and Sn and found a good agreement with experiment. Grimvall[94] estimated $\lambda$ for noble metals from Ziman's high temperature resistivity formula. Maksimov and Motulevich[95] followed the idea of Hopfield and estimated $\lambda$ from optical measurements for Pb, Sn, In, Al, Zn, Nb, V, Nb$_3$Sn, and V$_3$Ga, which are in good agreement with the McMillan's coupling constant $\lambda$ from superconductivity data.

In this Section, we show that weak localization leads to the same correction to the Boltzman conductivity as to McMillan's electron-phonon coupling constant $\lambda$ and $\lambda_{tr}$.

## 3.2.1 High Temperature resistivity

At high temperatures, the phonon limited electrical resistivity is given by[96-99]

$$
\begin{aligned}
\rho_{ph}(T) &= \frac{4\pi m k_B T}{ne^2\hbar} \int \frac{\alpha_{tr}^2 F(\omega)}{\omega} d\omega, \\
&= \frac{2\pi m k_B T}{ne^2\hbar} \lambda_{tr},
\end{aligned}
\tag{3. 3}
$$

where $\alpha_{tr}$ includes an average of a geometrical factor $1 - cos\theta_{\vec{k}\vec{k}'}$ and $F(\omega)$ is the phonon density of states. On the other hand, in the strong-coupling theory of superconductivity,[14,66] McMillan's electron-phonon coupling constant is defined by[66]

$$
\lambda = 2 \int \frac{\alpha^2(\omega)F(\omega)}{\omega} d\omega.
\tag{3. 4}
$$

Assuming $\alpha_{tr}^2 \cong \alpha^2$,[96,100-102] we obtain

$$\rho_{ph}(T) = \frac{2\pi m k_B T}{ne^2 \hbar}\lambda_{tr} \qquad (3.\ 5)$$

$$\cong \frac{2\pi m k_B T}{ne^2 \hbar}\lambda. \qquad (3.\ 6)$$

Consequently McMillan's coupling constant $\lambda$ determines also size and sign of TCR.

The existence of this relationship was confirmed theoretically and experimentally. Table 3.1 shows the comparison of $\lambda_{tr}$ and $\lambda$ by Economou[100] for various materials. He obtained $\lambda_{tr}$ from Eq. (3.5) and compared with $\lambda$, as obtained from $T_c$ measurements, and/or tunneling experiments, and/or first principle calculations.[101] The overall agreement between $\lambda_{tr}$ and $\lambda$ is impressive. Grimvall estimated $\lambda$ for noble metals[94] and noble metal alloys[103] from Eq. (3.6). Maksimov[102] also noted the direct relation between $\lambda$ and high temperature resistivity. Hayman and Carbotte[104] pointed out that information on the volume dependence of electron-phonon coupling strength can be obtained from high temperature resistivity. Chakraborty, Pickett, and Allen[105] used Eq. (3.5) to obtain empirical values of $\lambda_{tr}$ for Nb, Mo, Ta, and W. They found that $\lambda_{tr}$ from resistance and McMillan's coupling constant $\lambda$ from superconductivity are very similar in magnitude for these materials. We can also mention experimental confirmations by Rapp and Crawfoord[106] for Nb-V alloys, by Rapp and Fogelholm[107] for Al-Mg alloys, by Flükiger and Ishikawa[108] for Zr-Nb-Mo alloys, by Fogelholm and Rapp[109] for In-Sn alloys, by Lutz et al.[110] for Nb$_3$Ge films, by Man'kovskii et al.[111] for thin Sn films, by Rapp, Mota and Hoyt[112] for Au-Ga alloys, and by Sundqvist and Rapp[113] for aluminum under pressure. Figure 3.3 shows McMillan's coupling constant $\lambda$ versus $d\rho/dT$ for Au-Ga, Au-Al, and Ag-Ga alloys,[114] which exemplifies the correlation implied by Eq. (3.6).
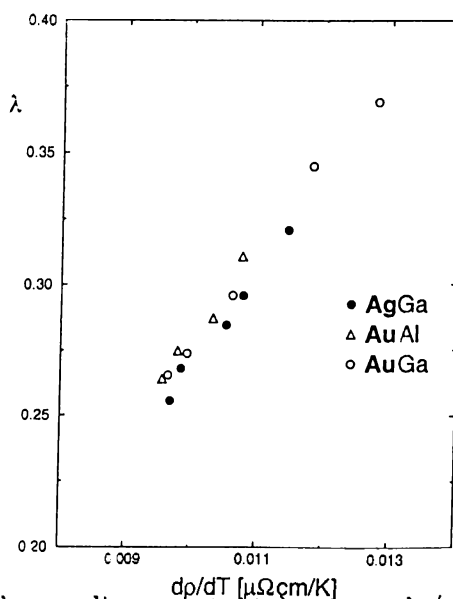
Figure 3. 3: McMillan's coupling constant $\lambda$ versus $d\rho/dT$. Data are from Rapp, Ref. 114 and Ref. 96

| Metal | $\lambda_{tr}$ | $\lambda$ | Metal | $\lambda_{tr}$ | $\lambda$ |
|-------|------|--------|-------|------|--------|
| Li | .40 | .41±.15 | Na | .16 | .16±.04 |
| K | .14 | .13±.03 | Rb | .19 | .16±.04 |
| Cs | .26 | .16±.06 | Mg | .32 | .35±.04 |
| Zn | .67 | .42±.05 | Cd | .51 | .40±.05 |
| Al | .41 | .43±.05 | Pb | 1.79 | 1.55 |
| In | .85 | .805 | Hg | 2.3 | 1.6 |
| Cu | .13 | .14±.03 | Ag | .13 | .10±.04 |
| Au | .08 | .14±.05 | Nb | 1.11 | .9±.2 |

Table 3.1: Comparison of $\lambda_{tr}$ and $\lambda$ as given in Ref. 100 and Ref. 101

## 3.2.2 Weak localization correction to McMillan's coupling constant $\lambda$ and $\lambda_{tr}$

Now we need to calculate McMillan's electron-phonon coupling constant $\lambda$ for highly disordered systems. We use McMillan's version of the strong-coupling theory.[66,71] (For simplicity we consider an Einstein model with frequency $\omega_D$). Note that $\lambda$ can be written as[66]

$$\lambda = 2 \int \frac{\alpha^2(\omega)F(\omega)}{\omega} d\omega \qquad (3.\ 7)$$

$$= N_0 \frac{< I^2 >}{M < \omega^2 >}, \tag{3.8}$$

where $M$ is the ionic mass and $N_0$ is the electron density of states at the Fermi level. $< I^2 >$ is the average over the Fermi surface of the square of the electronic matrix element and $< \omega^2 > = \omega_D^2$. In the presence of impurities, weak localization leads to a correction to $\alpha^2(\omega)$ or $< I^2 >$, (disregarding the changes of $F(\omega)$ and $N_0$).

The equivalent electron-electron potential in the electron-phonon problem is given by the phonon Green's function $D(x - x')$:[115,116]

$$V(x - x') \rightarrow \frac{I_0^2}{M\omega_D^2} D(x - x'), \tag{3.9}$$

where $x = (\mathbf{r}, t)$ and $I_0$ is the electronic matrix element for the plane wave states. The Fröhlich interaction at finite temperatures is then obtained by[117]

$$
\begin{aligned}
V_{nn'}(\omega, \omega') &= \frac{I_0^2}{M\omega_D^2} \int \int d\mathbf{r} d\mathbf{r}' \psi_{n'}^*(\mathbf{r}) \psi_{\bar{n}'}^*(\mathbf{r}') D(\mathbf{r} - \mathbf{r}', \omega - \omega') \psi_{\bar{n}}(\mathbf{r}') \psi_n(\mathbf{r}) \\
&= \frac{I_0^2}{M\omega_D^2} \int |\psi_{n'}(\mathbf{r})|^2 |\psi_n(\mathbf{r})|^2 d\mathbf{r} \frac{\omega_D^2}{\omega_D^2 + (\omega - \omega')^2} \\
&= V_{nn'} \frac{\omega_D^2}{\omega_D^2 + (\omega - \omega')^2}, \tag{3.10}
\end{aligned}
$$

where

$$
\begin{aligned}
D(\mathbf{r} - \mathbf{r}', \omega - \omega') &= \sum_{\vec{q}} \frac{\omega_D^2}{(\omega - \omega')^2 + \omega_D^2} e^{i\vec{q} \cdot (\mathbf{r} - \mathbf{r}')} \\
&= \frac{\omega_D^2}{(\omega - \omega')^2 + \omega_D^2} \delta(\mathbf{r} - \mathbf{r}'). \tag{3.11}
\end{aligned}
$$

Here $\omega$ means the Matsubara frequency and $\psi_n$ and $\psi_{\bar{n}}$ denote the scattered state and its time-reversed partner, respectively. Therefore, we get the strong-coupling gap equation[71]

$$
\begin{aligned}
\Delta(n, \omega) &= T \sum_{\omega'} \sum_{n'} V_{nn'}(\omega, \omega') \frac{\Delta(n', \omega')}{\omega'^2 + E_{n'}^2(\omega')} \\
&= T \sum_{\omega'} \frac{\omega_D^2}{(\omega - \omega')^2 + \omega_D^2} \sum_{n'} V_{nn'} \frac{\Delta(n', \omega')}{\omega'^2 + E_{n'}^2(\omega')}, \tag{3.12}
\end{aligned}
$$

where

$$E_{n'}(\omega') = \sqrt{\epsilon_{n'}^2 + \Delta_{n'}^2(\omega')}, \qquad (3.\ 13)$$

and McMillan's electron-phonon coupling constant $\lambda$

$$\lambda = N_0 < V_{nn'}(0,0) >= N_0 \frac{I_0^2}{M\omega_D^2} < \int |\psi_n(\mathbf{r})|^2 |\psi_{n'}(\mathbf{r})|^2 d\mathbf{r} > . \qquad (3.\ 14)$$

Here $\epsilon_n$ means the eigenenergy of the scattered state $\psi_n$. It is remarkable that McMillan's electron-phonon coupling constant is determined by the density correlation function.

Note also that in the presence of impurities, the density correlation function has a free-particle form for $t < \tau$ (scattering time) and a diffusive form for $t > \tau$.[119] As a result, for $t > \tau$ (or $r > \ell$), one finds[119-123]

$$
\begin{aligned}
R(t > \tau) &= \int_{t>\tau} |\psi_n(\mathbf{r})|^2 |\psi_{n'}(\mathbf{r})|^2 d\mathbf{r} \\
&= \sum_{\vec{q}} |<\psi_n|e^{i\vec{q}\cdot\mathbf{r}}|\psi_{n'}>|^2 \\
&= \sum_{\pi/L<\vec{q}<\pi/\ell} \frac{1}{2\pi\hbar N_0 D\vec{q}^2} \qquad (3.\ 15) \\
&= \frac{3}{2(k_F\ell)^2}(1 - \frac{\ell}{L}). \qquad (3.\ 16)
\end{aligned}
$$

Here $\ell$ is the mean free path and $L$ is the inelastic diffusion length. Whereas the contribution from the free-particle-like density correlation for $t < \tau$ is[71,119]

$$
\begin{aligned}
R(t < \tau) &= \int_{t<\tau} |\psi_n(\mathbf{r})|^2 |\psi_{n'}(\mathbf{r})|^2 d\mathbf{r} \\
&= [1 - \frac{3}{(k_F\ell)^2}(1 - \frac{\ell}{L})]. \qquad (3.\ 17)
\end{aligned}
$$

Since the phonon-mediated interaction is retarded for $t_{ret} \sim 1/\omega_D$, only the free-particle-like density correlation contributes to $\lambda$. Consequently, we obtain weak localization correction to the McMillan's coupling constant

$$\lambda = N_0 \frac{I_0^2}{M\omega_D^2}[1 - \frac{3}{(k_F\ell)^2}(1 - \frac{\ell}{L})]. \qquad (3.\ 18)$$

and

$$
\begin{aligned}
\lambda_{tr} &= 2 \int \frac{\alpha_{tr}^2(\omega) F(\omega)}{\omega} d\omega \\
&\cong \frac{N_0 I_0^2}{M \omega_D^2} [1 - \frac{3}{(k_F \ell)^2}(1 - \frac{\ell}{L})] \\
&= \frac{N_0 I_0^2}{M \omega_D^2} [1 - \frac{3}{(k_F \ell)^2}].
\end{aligned}
\tag{3. 19}
$$

We have used the fact that $L$ is effectively infinite at $T = 0$. Note that the weak localization correction term is the same as that for the conductivity.

## 3.3    Explanation of the Mooij Rule

As noted in the Section II, a positive TCR is a high temperature phenomenon whereas a negative TCR is low temperature phenomenon. Then, the decrease of the positive TCR is mainly due to the decrease of the phonon-limited resistivity which is a manifestation of weak localization correction to the electron-phonon interaction. On the other hand, the negative TCR originates from the residual resistivity, which is also a manifestation of weak localization correction to the conductivity. Accordingly, weak localization seems to be the physical origin of the Mooij rule.

### 3.3.1    Decrease of TCR at high temperatures

Upon substituting Eq. (3.19) into Eq. (3.3), one finds the phonon-limited high temperature resistivity

$$
\begin{aligned}
\rho_{ph}(T) &\cong \frac{2\pi m k_B T}{n e^2 \hbar} \lambda \\
&\cong \frac{2\pi m k_B T}{n e^2 \hbar} \frac{N_0 I_0^2}{M \omega_D^2} [1 - \frac{3}{(k_F \ell)^2}].
\end{aligned}
\tag{3. 20}
$$

Note that as the disorder parameter $1/k_F \ell$ is increasing, both magnitude of the phonon-limited resistivity and TCR decrease. This behavior is due to the reduction of McMillan's electron-phonon coupling constant when electrons

are weakly localized. It is remarkable that the slope of the high temperature resistivity varies as $\sim 1/(k_F\ell)^2$, in accord with the behavior of the residual resistivity.

The phonon-limited resistivity $\rho_{ph}$ versus temperature T is shown in Fig. 3.4 (a) for six values of $k_F\ell$. We used $k_F = 0.8\mathring{A}^{-1}$, $n = k_F^3/3\pi^2$, and $N_0I_0^2/(M\omega_D^2) = 0.5$. It is clear that TCR is decreasing significantly as the electrons are weakly localized.
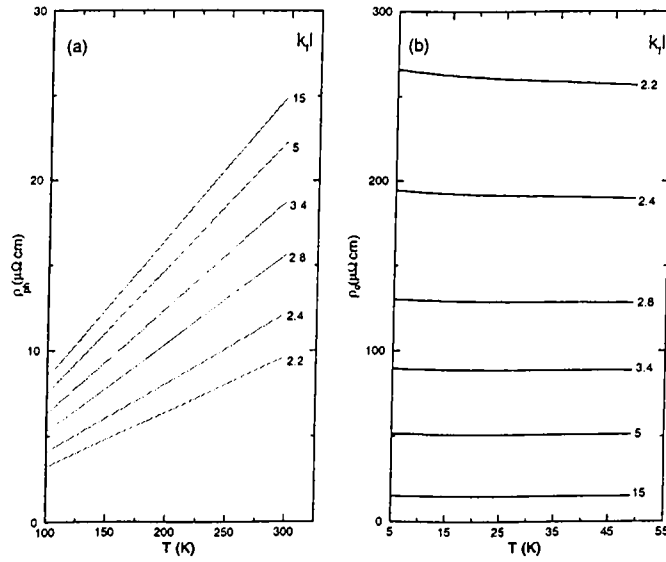


Figure 3. 4: (a) Phonon-limited resistivity $\rho_{ph}$ versus T for $k_F\ell = 15$, 5, 3.4, 2.8, 2.4, and 2.2. (b) residual resistivity $\rho_0$ versus T for the same six values of $k_F\ell$.

### 3.3.2 Negative TCR at low temperatures

At low temperatures conductivity and residual resistivity are given by

$$\sigma = \sigma_B[1 - \frac{3}{(k_F\ell)^2}(1 - \frac{\ell}{L})], \qquad (3.\ 21)$$

and

$$\rho_0 = \frac{1}{\sigma_B[1 - \frac{3}{(k_F\ell)^2}(1 - \frac{\ell}{L})]}, \qquad (3.\ 22)$$

where $\sigma_B = ne^2\tau/m$. When $1/k_F\ell$ becomes comparable to $\sim 1$, magnitude and slope of $\rho_{ph}(T)$ are becoming too small. In that case, only the residual

resistivity will play an important role. Therefore, the observed negative TCR may be understood from the residual part. With decreasing $T$, since the inelastic diffusion length $L$ increases, the residual resistivity will also increase, leading to the negative TCR. We stress that both the phonon-limited resistivity and the residual resistivity have the same quadratic dependence on the disorder parameter $1/k_F\ell$.

Figure 3.4 (b) shows the temperature dependence of the residual resistivity $\rho_0$ for $k_F\ell = 2.2, 2.4, 2.8, 3.4, 5$, and $15$. Since it is difficult to evaluate $k_F\ell$ up to a factor of 2,[124] we assumed that $\rho_0 = 100\mu\Omega cm$ corresponds to $k_F\ell = 3.2$. We used the same $k_F$ as in Fig. 3.4 (a) and $L = \sqrt{D\tau_i} = \sqrt{\ell} \times 350/T(\mathring{A})$. Here $D$ is the diffusion constant and $\tau_i$ denotes the inelastic scattering time. When $k_F\ell$ is comparable to 1, the negative TCR emerges. Notice the scale difference between Figures, 3.4 (a) and 3.4 (b).

### 3.3.3  Comparison with experiment

In Sections 3.3.1 and 3.3.2, the physical origin of the Mooij rule is explained. In this section, we compare our theoretical resistivity curve with experimental data (Figure 3.2) for an extended temperature range. Let us remind the approximate formula for $\rho(T)$ suggested by Lee and Ramakrishnan,[68] i.e.,

$$\rho(T) = \rho_0 + (\rho_M - \rho_0)AT. \tag{3.23}$$

This form of equation can be obtained by adding the residual resistivity Eq. (3.22) and the phonon-limited resistivity Eq. (3.20), that is,

$$\begin{aligned} \rho(T) &= \rho_0 + \rho_{ph}(T) \\ &= \frac{1}{\sigma_B[1 - \frac{3}{(k_F\ell)^2}(1 - \frac{\ell}{L})]} + \frac{2\pi m k_B T}{n e^2 \hbar} \frac{N_0 I_0^2}{M\omega_D^2}[1 - \frac{3}{(k_F\ell)^2}]. \end{aligned} \tag{3.24}$$

Note that the addition of both resistivities does not correspond to Matthiessen's rule. We included the interference effect between the electron-phonon and electron-impurity interactions:

$$\rho(T) = \rho_0 + \rho_{ph}(c = 0) + \Delta\rho_{ph}^{int}, \tag{3.25}$$

where $c$ denotes an impurity concentration. Whereas Altshuler[125] and Reizer and Sergeev[126] investigated corrections to the impurity resistivity due to interference, we considered its correction to the phonon-limited resistivity. Since the interference correction to the impurity resistivity is $\sim 1\%$ of the residual resistivity,[126,127] we neglect its effect for simplicity.

In general, the phonon-limited resistivity at any temperature $T$ is given by

$$\rho_{ph}(T) = \frac{4\pi m}{ne^2} \int \frac{(\beta\hbar\omega)\alpha_{tr}^2(\omega)F(\omega)}{(e^{\beta\hbar\omega} - 1)(1 - e^{-\beta\hbar\omega})} d\omega, \qquad (3.\ 26)$$

where $\beta = 1/k_B T$. For an Einstein phonon model with[128]

$$\alpha_{tr}^2(\omega)F(\omega) = \frac{N_0 I_0^2}{2M\omega_D}\delta(\omega - \omega_D), \qquad (3.\ 27)$$

it is rewritten as[129]

$$\rho_{ph}(T) = \frac{2\pi m}{ne^2} \frac{N_0 I_0^2}{M\omega_D^2} \frac{(\beta\hbar\omega_D)\omega_D}{(e^{\beta\hbar\omega_D} - 1)(1 - e^{-\beta\hbar\omega_D})}. \qquad (3.\ 28)$$

We stress that this result is exact for the phonon-limited resistivity in an Einstein model. Including the weak localization correction to $\alpha^2(\omega) \cong \alpha_{tr}^2(\omega)$,

$$\alpha_{tr}^2(\omega)F(\omega) = \frac{N_0 I_0^2}{2M\omega_D}[1 - \frac{3}{(k_F\ell)^2}]\delta(\omega - \omega_D), \qquad (3.\ 29)$$

one finds

$$\rho_{ph}(T) = \frac{2\pi m}{ne^2} \frac{N_0 I_0^2}{M\omega_D^2}[1 - \frac{3}{(k_F\ell)^2}]\frac{(\beta\hbar\omega_D)\omega_D}{(e^{\beta\hbar\omega_D} - 1)(1 - e^{-\beta\hbar\omega_D})}. \qquad (3.\ 30)$$

Finally, we obtain the total resistivity at any temperature $T$:

$$\begin{aligned}
\rho(T) &= \rho_0 + \rho_{ph}(T) \\
&= \frac{1}{\sigma_B[1 - \frac{3}{(k_F\ell)^2}(1 - \frac{\ell}{L})]} + \frac{2\pi m}{ne^2}\frac{N_0 I_0^2}{M\omega_D^2}[1 - \frac{3}{(k_F\ell)^2}]\frac{(\beta\hbar\omega_D)\omega_D}{(e^{\beta\hbar\omega_D} - 1)(1 - e^{-\beta\hbar\omega_D})} \qquad (3.\ 31)
\end{aligned}$$

(If we consider Debye and realistic phonon models, there are minor changes. However, the overall behavior is the same. More details will be published elsewhere.)

Figure 3.5 shows resistivity as a function of temperature for $k_F\ell =$ 2.3, 2.5, 2.8, 3.4, 5, and 15. Solid lines represent the resistivity from an accurate expression Eq. (3.31), while dashed lines are obtained from Eq. (3.24). We used the same parameters as those in Fig. 3.4 and $\hbar\omega_D = 250K$. It is noteworthy that both equations give rise to almost the same curve as the system is more disordered. For low temperatures $\tau_i$ is determined by electron-electron scattering while for high temperatures it is determined by electron-phonon scattering. Since we are interested in rather high temperatures, we assumed $\tau_i \sim T^{-1}$ corresponding to the electron-phonon scattering.[71,69] Despite the crudeness of the calculation, the overall behavior is in good agreement with experiment, Fig. 3.2.
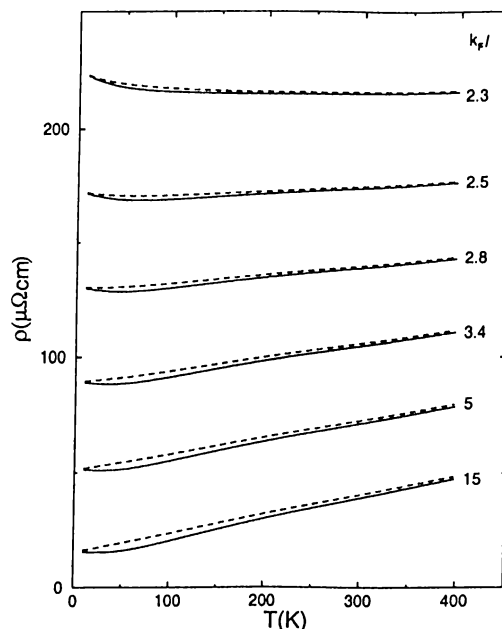


Figure 3. 5: Calculated resistivity versus temperature for $k_F\ell = 15$, 5, 3.4, 2.8, 2.5, and 2.3. The solid lines are $\rho(T)$ from an accurate formula, Eq. (3.31). The dashed lines represent the resistivity obtained from the approximate expression, Eq. (3.24).

## 3.4 Discussion

At low temperatures interference of the Coulomb interactions and impurity scattering leads to the interaction correction to the conductivity.[121,68] This effect is described by[130]

$$\sigma = \sigma_B[1 - \frac{3}{(k_F\ell)^2}(1 - \frac{\ell}{L}) - \frac{C}{(k_F\ell)^2}(1 - \frac{\ell}{L_T})], \qquad (3.\ 32)$$

where $L_T = (\hbar D/k_B T)^{1/2}$ and $C \sim 1$. The second correction term is the interaction term. The constant $C$, however, changes sign depending on exchange and Hartree terms and since it is difficult to determine $C$,[68,69,130] we didn't include this term. But it may be important at much lower temperatures.

It is clear that understanding of weak localization effects on the electron-phonon interaction requires further theoretical and experimental investigation. In particular, weak localization effects on the attenuation of sound waves, shear modulus, thermal resistance, and shift in phonon frequencies will be very interesting. Since superconductivity, too, is caused by the electron-phonon interactions, comparative studies of normal and superconducting properties of metallic samples will be beneficial. For instance, Testardi and coworkers[79−82] found an universal correlation between $T_c$ and resistance ratio. They also found that decreasing $T_c$ is accompanied by decrease of the thermal electrical resistivity.[82]

Note that this study may provide a means of probing the phonon-mechanism in exotic superconductors, such as, heavy fermion superconductors, organic superconductors, fullerene superconductors, and high $T_c$ cuprates. For superconductivity due to electron-phonon interaction we predict the following behavior. If the electrons are weakly localized due to impurities or radiation damage, electron-phonon interaction is weakened. As a result, both $T_C$ and TCR should decrease at the same rate. When $\lambda$ is approaching zero, both $T_c$ and TCR should drop to zero almost simultaneously. If this happens we may say that the electron-phonon interaction is the origin of the pairing in superconductors. Such a behavior has already been observed in A15 superconductors[79−82] and Ternary superconductors.[131]

# Chapter 4

# Conclusion

The effect of magnetic impurities in crystalline and amorphous states of superconductors has been studied theoretically. The *pure limit behavior* in crystalline Cd observed by Roden and Zimmermeyer and the decrease of the initial slope of the $T_c$ depression due to disorder have been explained. In particular, the initial slope of the $T_c$ decrease is decreasing by a factor $\sqrt{\ell/\xi_0}$ as the system is getting disordered. We suggest that a more systematic experimental investigation of the different behavior of the magnetic impurities in crystalline and amorphous superconductors is necessary. Such an investigation may also be important for understanding whether a transition metal impurity possesses a magnetic moment in a metallic host or not.

It is also shown that weak localization decreases both conductivity and electron-phonon interaction at the same rate and thereby leads to the Mooij rule. As the residual resistivity is increasing due to weak localization, the thermal electrical resistivity is decreasing, producing the decrease of TCR. When the electron-phonon interaction is near zero, only the residual resistivity is left and therefore the negative TCR is obtained. This study may provide a means of probing the phonon-mechanism in exotic superconductors, such as, heavy fermion superconductors, organic and fullerene superconductors, and high $T_c$ superconductors.

41

# Bibliography

[1] R. D. Parks, ed., *Superconductivity*, (Marcel Dekker, NewYork, 1969).

[2] J. L. Schrieffer, *Theory of Superconductivity*, (Benjamin/Cummings, New York, 1983).

[3] M. Tinkham, *Introduction to Superconductivity*, (McGraw-Hill, New York, 1975).

[4] P. G. de Gennes, *Superconductivity of Metals and Alloys*, (Benjamin, New York, 1966).

[5] Jeffrey W. Lynn, ed., *High TemperatureSuperconductivity*, (Springer-Verlag, New York, 1990).

[6] H. Kamerlingh Onnes, Akad. van Wetenschappen (Amsterdam) **14**, 113 (1911).

[7] W. Meissner and R. Ochsenfeld, Naturwiss. **21**, 787(1933).

[8] D. Saint James, E. D. Thomas, and G. Sarma, *Type II Superconductivity*, (Pergamon, Oxford, 1969).

[9] F. London and H. London, Proc. Roy. Soc. (London) A **149**, 71 (1935).

[10] A. B. Pippard, Proc. Roy. Soc. (London) A **203**, 98 (1950).

[11] V. L. Ginzburg and L. D. Landau, Zh. Eksperim. i. Teor. Fiz. **20**, 1064 (1950).

[12] H. Fröhlich, Proc. Roy. Soc. (London) A **215**, 291 (1952).

[13] J. Bardeen, L. N. Cooper, and J. R. Schrieffer, Phys. Rev. **108**, 1175 (1957).

[14] G. M. Eliashberg, Sov. Phys. JETP **11**, 696 (1960).

[15] L. P. Gor'kov, Sov. Phys. JETP **7**, 505 (1958).

[16] P. G. de Gennes, *Superconductivity of Metals and Alloys*, (Benjamin, New York, 1966), ch. 5.

[17] J. G. Bednorz and K. A. Müller, Z. Phys. B **64**, 189 (1986).

[18] R. C. Dynes, A. E. White, J. M. Graybeal, and J. P. Garno, Phys. Rev. Lett. **57**, 2195 (1986).

[19] J. M. Graybeal, P. M. Mankiewich, R. C. Dynes, and M. R. Beasley, Phys. Rev. Lett. **59**, 2697 (1987).

[20] K. K. Likharev, Rev. Mod. Phys. **51**, 101 (1979).

[21] Yong-Jihn Kim and A. W. Overhauser, Phys. Rev. B **47**, 8025 (1993).

[22] Yong-Jihn Kim and A. W. Overhauser, Phys. Rev. B **49**, 15799 (1994).

[23] Yong-Jihn Kim, Mod. Phys. Lett. B **10**, 555 (1996).

[24] P. W. Anderson, J. Phys. Chem. Solids **11**, 26 (1959).

[25] G. Grimwall, *The Electron Phonon Interaction in Metals*, (North-Holland, Amsterdam, 1981), p. 4.

[26] J. H. Mooij, Phys. Status Solidi A **17**, 521 (1973).

[27] M. F. Merriam, S. H. Liu, and D. P. Seraphim, Phys. Rev. **136**, A17 (1964).

[28] G. Boato, G. Gallinaro, and C. Rizzuto, Phys. Rev. **148**, 353 (1966).

[29] E. Wassermann, Z. Phys. **220**, 6 (1969).

[30] W. Bauriedl and G. Heim, Z. Phys. B **26**, 29 (1977).

[31] M. Hitzfeld and G. Heim, Solid State Commun. **29**, 93 (1979).

[32] B. Roden and G. Zimmermeyer, J. Low Temp. Phys. **25**, 267 (1976).

[33] W. Schlabitz and P. Zaplinski, in *Proc. of 14th Int. Conf. Low Temp. Phys. Helsinki*, 1975, Vol. 3, p. 452.

[34] A. Hofmann, W. Bauriedl, and P. Ziemann, Z. Phys. B **46**, 117 (1982).

[35] T. Habisreuther, W. Miehle, A. Plewnia, and P. Ziemann, Phys. Rev. B **46**, 14566 (1992).

[36] W. Buckel, *Superconductivity: Fundamentals and Applications*, (VCH, Weinheim, 1991), p. 212.

[37] Mi-Ae Park, M. H. Lee, and Yong-Jihn kim, Physica C **306**, 96 (1998).

[38] A. A. Abrikosov and L. P. Gor'kov, Zh. Eksp. Teor. Fiz. **39**, 1781 (1961) [Sov. Phys. JETP **12**, 1243 (1961)].

[39] H. Falke, H. P. Jablonski, J. Kästner, and E. F. Wassermann, Z. Phys. **259**, 135 (1973).

[40] G. Boato, G. Gallinaro, and C. Rizzuto, Rev. Mod. Phys. **36**, 162 (1964).

[41] D. L. Martin, Phys. Rev. **167**, 640 (1968).

[42] W. Smith, J. Low Temp. Phys. **5**, 683 (1971).

[43] H. Sanchez, Thesis, Rutgers University, New Bruinswick, N. J., (1972).

[44] F. T. Hedgcock and C. Rizzuto, Phys. Lett. **24** A, 17 (1966).

[45] P. J. Ford, C. Rizzuto, and C. Salamoni, Phys. Rev. B **6**, 1851 (1972).

[46] J. V. Porto and J. M. Parpia, Phys. Rev. Lett. **74**, 4667 (1995).

[47] D.T. Sprague, T. M. Haard, J. B. Kycia, M. R. Rand, Y. Lee, P. S. Harrot, and W. P. Halperin, Phys. Rev. Lett. **75**, 661 (1995).

[48] K. Matsumodo, J. V. Porto, L. Pollack, E. N. Smith, T. L. Ho, and J. M. Parpia, Phys. Rev. Lett. **79**, 253 (1997).

[49] M. B. Maple, J. Appl. Phys. **9**, 179 (1976).

[50] M. A. Jensen anf H. Suhl, in *Magnetism: A Treatise on Modern Theory and Materials*, edited by G. T. Rado and H. Suhl (Academic, New York, 1966), Vol. II B, p. 183.

[51] K. Schwidtal, Z. Phys. **158**, 563 (1960).

[52] N. Barth, Z. Phys. **148**, 646 (1957).

[53] W. Buckel, M. Dietrich, G. Heim. and J. Kessler, Z. Phys. **245**, 283 (1971).

[54] A. Schertel, Phys. Verh. **2**, 102 (1951).

[55] P. Ziemann, Festkörperprobleme **XXIII**, 93 (1983).

[56] W. Opitz, Z. Phys. **141**, 263 (1955); A. W. Bjerkaas, D. M. Ginsberg, and B. J. Mostik, Phys. Rev. B **5**, 854 (1972).

[57] F. Reif and M. A. Woolf, Phys. Rev. Lett. **9**, 315 (1962).

[58] B. T. Matthias, H. Suhl, and E. Corenzwit, Phys. Rev. Lett. **1**, 92 (1958).

[59] K. Schwidtal, Z. Phys. **169**, 564 (1962).

[60] F. T. Hedgcock, S. N. Mahajan, and C. Rizzuto, J. Appl. Phys. **39**, 851 (1968).

[61] G. Zimmermeyer and B. Roden, Z. Phys. B **24**, 377 (1976).

[62] P. G. de Gennes, *Superconductivity of Metals and Alloys* (Benjamin, New York, 1966), ch. 4.

[63] P. W. Anderson and P. Morel, Phys. Rev. **123**, 1911 (1961).

[64] C. G. Granqvist and T. Claeson, J. Low Temp. Phys. **10**, 735 (1973).

[65] C. Kittel, *Introduction to Solid State Physics* (John Wiley, New York. 1976), chs. 5 and 6.

[66] W. L. McMillan, Phys. Rev. B **167**, 331 (1968).

[67] E. Abrahams, P. W. Anderson, D. C. Licciardello, and T. V. Ramakrishnan, Phys. Rev. Lett. **42**, 673 (1979).

[68] P. A. Lee and T. V. Ramakrishnan, Rev. Mod. Phys. **57**, 287 (1985).

[69] N. F. Mott and M. Kaveh, Adv. Phys. **34**, 329 (1985).

[70] Yong-Jihn Kim, Int. J. Mod. Phys. Lett. B **11**, 1731 (1997).

[71] Mi-Ae Park and Yong-Jihn Kim, Phys. Rev. B **61**, 14733 (2000).

[72] K. E. Kihlstrom, D. Mael, and T. H. Geballe, Phys. Rev. B **29**, 150 (1984).

[73] D. A. Rudman and M. R. Beasley, Phys. Rev. B **30**, 2590 (1984).

[74] C. C. Tsuei, S. von Molnar, and J. M. Coey, Phys. Rev. Lett. **41**, 664 (1978).

[75] R. A. Pollak, C. C. Tsuei, and R. W. Johnson, Solid State Commun. **23**, 879 (1977).

[76] A. T. Fiory and A. F. Hebard, Phys. Rev. Lett. **52**, 2057 (1984).

[77] H. Wiesmann, M. Gurvitch, A. K. Ghosh, H. Lutz, K. W. Jones, A. N. Goland, and M. Strongin, J. Low. Temp. Phys. **30**, 513 (1978).

[78] T. P. Orlando, E. J. McNiff, Jr., S. Foner, and M. R. Beasley, Phys. Rev. B **19**, 4545 (1979).

[79] J. M. Poate, L. R. Testardi, A. R. Storm, and W. M. Augustyniak, Phys. Rev. Lett. **35**, 1291 (1975).

[80] L. R. Testardi, R. L. Meek, J. M. Poate, W. A. Royer, A. R. Storm, and J. H. Wernick, Phys. Rev. B **11**, 4304 (1975).

[81] J. M. Poate, R. C. Dynes, L. R. Testardi, and R. H. Hammond, Phys. Rev. Lett. **37**, 1308 (1976).

[82] L. R. Testardi, J. M. Poate, and H. J. Levinstein, Phys. Rev. B. **15**, 2570 (1977).

[83] D. Pines, *Elementary Excitations in Solids*, (Benjamin, New York, 1963), ch. 5.

[84] M. Jonson and S. M. Girvin, Phys. Rev. Lett. **43**, 1447 (1979).

[85] Y. Imry, Phys. Rev. Lett. **44**, 469 (1980).

[86] M. Kaveh and N. F. Mott, J. Phys. C: Solid State Phys. **15**, L707 (1982).

[87] D. Belitz and W. Götze, J. Phys. C **15**, 981 (1982).

[88] D. Belitz and W. Schirmacher, J. Non-cryst. Solids **61/62**, 1073 (1983).

[89] N. F. Mott, *Conduction in Non-Crystalline Materials*, (Oxford University Press, Oxford, 1987), p.15.

[90] A. M. Jayannavar and N. Kumar, Phys. Rev. B **37**, 573 (1988).

[91] G. Gladstone, M. A. Jensen, and J. R. Schrieffer, in *Superconductivity*, Vol. 2, R. D. Parks ed. (Marcel Dekker, New York, 1969), p. 665.

[92] J. J. Hopfield, Comments Sol. Sta. Phys. **3**, 48 (1970).

[93] J. J. Hopfield, in *Superconductivity in d- and f-Band Metals*, D. H. Douglass ed. (AIP, New York, 1972), p. 358.

[94] G. Grimvall, Phys. Kondens. Materie **11**, 279 (1970).

[95] E. G. Maksimov and G. P. Motulevich, Zh. Eksp. Teor. Fiz. **61**, 414 (1971) [Sov. Phys. JETP **34**, 219 (1972)].

[96] G. Grimvall, *The Electron-Phonon Interaction in Metals*, (North-Holland, Amsterdam, 1981).

[97] B. Hayman and J. P. Carbotte, Can. J. Phys. **49**, 1952 (1971).

[98] B. Hayman and J. P. Carbotte, J. Phys. F **1**, 828 (1971).

[99] P. B. Allen, Phys. Rev. B **3**, 305 (1971).

[100] E. N. Economou, in *Metal Hydrides*, G. Bambakidis ed. (Plenum, New York, 1981), p. 1.

[101] G. Grimvall, Phys. Scripta, **14**, 63 (1976).

[102] E. G. Maksimov, Zh. Eksp. Teor. Fiz. **57**, 1660 (1969) [Sov. Phys. JETP **30**, 897 (1970)].

[103] G. Grimvall, Phys. Kondens. Materie **14**, 101 (1972).

[104] B. Hayman and J. P. Carbotte, Solid State Commun. **15**, 65 (1974).

[105] B. Chakraborty, W. E. Pickett, and P. B. Allen, Phys. Rev. B **14**, 3227 (1976).

[106] Ö. Rapp and C. Crawfoord, Phys. Stat. Sol. (b) **64**, 139 (1974).

[107] Ö. Rapp and R. Fogelholm, J. Phys. F: Metal Phys., **5**, 1694 (1975).

[108] R. Flükiger and M. Ishikawa, in Proceedings of the 14th International Conference on Low Temperature Physics, vol. 2, M. Krusius and M. Vuorio, eds. (North-Holland and Elsevier, Helsinki, 1975) p. 63.

[109] R. Fogelholm and Ö. Rapp, in Proceedings of the 14th International Conference on Low Temperature Physics, vol. 2, M. Krusius and M. Vuorio, eds. (North-Holland and Elsevier, Helsinki, 1975) p. 429.

[110] H. Lutz, H. Weismann, O. F. Kammerer, and M. Strongin, Phys. Rev. Lett. **36**, 1576 (1976).

[111] K. K. Man'kovskii, V. V. Pilipenko, Y. F. Komnik, and I. M. Dmitrenko, Zh. Eksp. Teor. Fiz. **59**, 740 (1970) [Sov. Phys. JETP **32**, 404 (1971)].

[112] Ö. Rapp, A. C. Mota, and R. F. Hoyt, Solid State Commun. **25**, 855 (1978).

[113] B. Sundqvist and Ö. Rapp, J. Phys. F: Metal Phys., **9**, 1694 (1979).

[114] Ö. Rapp, (1980), unpublished data quoted in Ref. 32, p. 252.

[115] A. A. Abrikosov, L. P. Gor'kov, and I. E. Dzyaloshinski, *Methods of Quantum Field Theory in Statistical Physics*, (Dover, New York, 1975), p. 79.

[116] A. Fetter and J. D. Walecka, *Quantum Theory of Many-Particle Systems*, (McGraw-Hill, New York, 1971), p. 401.

[117] W. Jones and N. H. March, *Theoretical Solid State Physics*, (Dover, New York, 1973), p. 897.

[118] P. W. Anderson, K. A. Muttalib, and T. V. Ramakrishnan, Phys. Rev. B **28**, 117 (1983).

[119] M. Kaveh, Phil. Mag. B **51**, 453 (1985).

[120] W. L. McMillan, Phys. Rev. B **24**, 2739 (1981).

[121] B. L. Altshuler and A. G. Aronov, Zh. Eksp. Teor. Fiz. **77**, 2028 (1979) [Sov. Phys. JETP **50**, 968 (1979)].

[122] E. Abrahams, P. W. Anderson, P. A. Lee, and T. V. Ramakrishnan, Phys. Rev. B **24**, 6783 (1981).

[123] Y. Imry, Y. Gefen, and D. J. Bergman, Phys. Rev. B **26**, 3436 (1982).

[124] H. Gutfreund, M. Weger, and O. Entin-Wohlman, Phys. Rev. B **31**, 606 (1985).

[125] B. L. Altshuler, Zh. Eksp. Teor. Fiz. **75**, 1330 (1978) [Sov. Phys. JETP **48**, 670 (1978)].

[126] M. Yu. Reizer and A. V. Sergeev, Zh. Eksp. Teor. Fiz. **92**, 2291 (1987) [Sov. Phys. JETP **65**, 1291 (1987)].

[127] P. M. Echternach, M. E. Gershenson, and H. M. Bozler, Phys. Rev. B **47**, 13659 (1993).

[128] S. V. Vonsovsky, Y. A. Izyumov, and E. Z. Kurmaev, *Superconductivity of Transition Metals*, (Springer-Verlag, Berlin, 1982), Chap. 2.

[129] H.-L. Engquist, Phys. Rev. B **21**, 2067 (1980).

[130] N. F. Mott, *Metal-Insulator Transitions*, (Taylor & Francis Ltd, London, 1990), p. 152 .

[131] R. C. Dynes, J. M. Rowell, and P. H. Schmidt, in *Ternary Superconductors*, ed. G. K. Shenoy, B. D. Dunlap, and F. Y. Fradin (North-Holland, Amsterdam, 1981), p. 169.